

UNCLASSIFIED

AD NUMBER
AD492301
NEW LIMITATION CHANGE
TO Approved for public release, distribution unlimited
FROM Distribution authorized to U.S. Gov't. agencies and their contractors; Administrative/Operational Use; MAY 1950. Other requests shall be referred to US Navy Office of Naval Research, Washington, DC.
AUTHORITY
ONR notice, 27 Jul 1971

THIS PAGE IS UNCLASSIFIED

**UNCLASSIFIED**

**AD** 492301

**DEFENSE DOCUMENTATION CENTER**

**FOR**

**SCIENTIFIC AND TECHNICAL INFORMATION**

**CAMERON STATION ALEXANDRIA, VIRGINIA**



**UNCLASSIFIED**

**NOTICE:** When government or other drawings, specifications or other data are used for any purpose other than in connection with a definitely related government procurement operation, the U. S. Government thereby incurs no responsibility, nor any obligation whatsoever; and the fact that the Government may have formulated, furnished, or in any way supplied the said drawings, specifications, or other data is not to be regarded by implication or otherwise as in any manner licensing the holder or any other person or corporation, or conveying any rights or permission to manufacture, use or sell any patented invention that may in any way be related thereto.

**Best  
Available  
Copy**

*Unannounced*

AD - <b>492301</b>	REPORT CLASSIFICATION <b>(U)</b> C S RD
SOURCE (to be supplied by DDC) <i>California Institute of Technology Dept. of Engineering</i>	
TITLE (unclassified only) <i>Investigation of Atmospheric Diffusion Processes By Means of Experimental, Analytical, and Numerical Techniques</i>	
REPORT IDENTIFICATION	REPORT DATE/S <i>May '50</i>
CONTRACT NO. <i>N60nc 2756</i>	
DDC FORM 0-29 INTERIM SOURCE AUTHORITY	
DUPE CHECKER'S INITIALS <i>P/C</i>	

ADDITIONAL INFO		
DDCI	WHITE SECTION <input type="checkbox"/>	
DDC	DDP SECTION <input type="checkbox"/>	
REARRANGED		
SUBSTITUTION		
DISTRIBUTION/AVAILABILITY CODES		
DIST.	AVAIL.	SPECIAL
<i>2</i>		

11  
11  
11

11  
11  
11

UNIVERSITY OF CALIFORNIA  
DEPARTMENT OF ENGINEERING  
LOS ANGELES

072 260

⑥ INVESTIGATION OF  
ATMOSPHERIC DIFFUSION PROCESSES  
BY MEANS OF  
EXPERIMENTAL, ANALYTICAL, AND NUMERICAL  
TECHNIQUES

⑩ H. F. POPPENDIEK  
J. E. VEHRENCAMP

Work Sponsored by Office of Naval Research  
(Geophysical Branch)  
Navy Department, Washington, D.C.

Contract <sup>⑮</sup> N6-ONR-275

Task Order  
⑬ NR-082-036

⑰ 6

L. M. K. BOELTER, CHAIRMAN OF THE DEPARTMENT OF ENGINEERING

⑪ MAY 1950

⑫ 54P

*esp*

*mt*

TABLE OF CONTENTS .

Summary	1
Nomenclature	2
Introduction	6
Basic Eddy Diffusion Relations	8
Experimental Techniques of Determining Eddy Diffusivities, Thermal Conductances, and Drag Coefficients	10
A. Convective Heat Transfer	10
B. Momentum Transfer	12
Analytical and Numerical Eddy Diffusion Analyses	16
A. Analytical Analyses	16
B. Numerical Analyses	25
Analysis of Several Sets of Micrometeorological Data	28
A. Experimental Determination of Convective Heat Flows, Convective Conductances, Shear Stresses, Drag Coefficients, and Eddy Diffusivities	28
1. Heat Transfer	28
2. Momentum Transfer	29
B. Numerical Eddy Diffusion Analyses of Transient Air Temperature Data	37
C. Eddy Diffusion Analyses Found in the Literature	41
DISCUSSION	45
ACKNOWLEDGMENTS	49
APPENDIX	50
REFERENCES	52

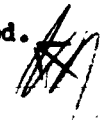
SUMMARY


<sup>The</sup>  
~~This~~ paper concerns ~~itself~~ an investigation of the atmospheric diffusion processes by means of experimental, analytical, and numerical methods.

Experimental momentum transfer and heat transfer analyses are presented. Shear stresses in the surface layer are measured directly by means of a shear meter; momentum eddy diffusivities and drag coefficients over flat ground are determined from shear stress and wind velocity data. Convective heat transfer rates in the surface layer are measured indirectly by means of a heat flow meter and a radiometer; convective conductances are determined from the convective heat flow and air temperature data.

Two new, analytical, periodic, convective heat flow solutions for the atmospheric system are derived. One solution pertains to an eddy diffusion system in which the boundary temperature varies sinusoidally with time and the eddy diffusivity varies sinusoidally with time but is independent of height. The other solution pertains to an eddy diffusion system in which the boundary temperature varies sinusoidally with time and the eddy diffusivity varies sinusoidally with time and linearly with height.

A simple heat-momentum transfer analogy for the surface layer <sup>was</sup> ~~has been~~ developed which relates some of the pertinent heat and momentum transfer variables in the atmospheric diffusion system.

Three numerical methods of determining eddy diffusivities as a function of time and height from transient air temperature and humidity profiles are presented. 





## NOMENCLATURE

English Letters

$a_n$	coefficients of the Fourier cosine series, equation (22), $^{\circ}\text{F}$
$A_s$	shear meter surface area exposed to air flow, $\text{ft}^2$
$b_1$	constant in equation (31), $\text{ft}^2/\text{hr}$
$b_2$	constant in equation (31), $\text{ft}/\text{hr}$
$b_3$	constant in equation (31), dimensionless
$B(\beta)$	function of $\beta$ defined in equation (42)
$C$	constant in equation (24)
$C_n$	coefficients in equation (25), $^{\circ}\text{F}$
$C'$	water vapor concentration, $\#/ \text{ft}^3$
$C_D$	drag coefficient
$c_1, c_2$	constants in equation (14), $\text{ft}^2/\text{hr}$
$c_p$	fluid heat capacity, $\text{Btu}/\# \text{ } ^{\circ}\text{F}$
$E$	constant in equation (43)
$E_0$	constant in equation (47)
$e_n$	coefficients in equation (48), $^{\circ}\text{F}$
$e$	base of natural logarithms
$f_0$	unit thermal convective conductance, $\text{Btu}/\text{hr ft}^2 \text{ } ^{\circ}\text{F}$
$F_D$	drag force on the shear meter, $\#$
$g$	acceleration of gravity, $\text{ft}/\text{hr}^2$
$g_n$	coefficients in the Fourier cosine series, equation (39), $^{\circ}\text{F}$
$H_0^{(1)}$	Hankel function of the zero order
$i$	$\sqrt{-1}$
$j$	ratio of the vertical eddy diffusivity for mass transfer to the vertical eddy diffusivity for heat transfer
$k$	thermal conductivity of air, $\text{Btu}/\text{hr ft}^2 ({}^{\circ}\text{F}/\text{ft})$
$k_s$	spring constant, $\text{lbs}/\text{inch}$
$K$	Karman constant
$l$	latent heat of vaporisation of water, $\text{Btu}/\#$

$M_0$	modulus of the complex function $H_0^{(n)}$
$n$	positive integer
$P$	constant in equation (43)
$P_n$	constants in equation (48), 1/hr
$\left(\frac{q}{A}\right)_{conv}$	vertical convective heat transfer rate per unit area, Btu/hr ft <sup>2</sup>
$\left(\frac{q}{A}\right)_{conv,0}$	vertical convective heat transfer rate per unit area at the ground, Btu/hr ft <sup>2</sup>
$\left(\frac{q}{A}\right)_{e,0}$	heat transfer rate per unit area due to evaporation or condensation of water vapor at the interface, Btu/hr ft <sup>2</sup>
$\left(\frac{q}{A}\right)_{gaseous}$	heat transfer rate per unit area due to radiation from water vapor, CO <sub>2</sub> , and dust in the atmosphere, Btu/hr ft <sup>2</sup>
$\left(\frac{q}{A}\right)_{g,0}$	heat transfer rate per unit area into or out of the ground at the interface, Btu/hr ft <sup>2</sup>
$\left(\frac{q}{A}\right)_{g.r.}$	ground radiosity per unit area (emitted and reflected radiation), Btu/hr ft <sup>2</sup>
$\left(\frac{q}{A}\right)_{solar}$	solar irradiation per unit area, Btu/hr ft <sup>2</sup>
$\left(\frac{q}{A}\right)_{t.a.,0}$	total hemispherical radiation per unit area at the ground, Btu/hr ft <sup>2</sup>
$r$	a variable defined by equation (40), ft/(hr) <sup>1/2</sup>
$R(r)$	a function of $r$ defined by equation (42)
$s$	an angle whose tangent is described for equation (50)
$t$	potential temperature, equal to $T + \Gamma z$ , °F
$t_0$	amplitude of the sinusoidal boundary temperature wave, °F
$T_l$	mean air temperature at the laminar sublayer - turbulent layer interface (see Figure 15), °F
$T_r$	mean air temperature at the reference height, $z_r$ , °F
$T_s$	mean air-earth interface temperature, °F
$U, V, W$	mean fluid velocities in the $x$ , $y$ , and $z$ directions, respectively, ft/hr
$U_l$	mean air velocity at the laminar sublayer - turbulent layer interface, ft/hr
$U_r$	mean air velocity at the reference height, $z_r$ , ft/hr
$x, y, z$	the cartesian coordinates (the earth's surface is in the $xy$ plane), ft

$z_1$	laminar sublayer thickness, ft
$z_0$	roughness parameter, ft
$Z(z)$	a function of $z$ defined by equation (23)

#### Greek Letters

$\alpha_g$	grey body earth surface emissivity
$\alpha'$	ratio of the vertical eddy diffusivity for heat transfer to the vertical eddy diffusivity for momentum transfer
$\beta$	a variable defined by equation (33), hr
$\Gamma$	adiabatic lapse rate, $^{\circ}\text{F}/\text{ft}$
$\gamma$	air density, $\#/ft^3$
$\delta_s$	spring deflection, inches
$\epsilon_{x'} \epsilon_{y'} \epsilon_{z'}$	thermal eddy diffusivities in the $x$ , $y$ , and $z$ directions, $ft^2/\text{hr}$
$\epsilon_{Mass}$	vertical eddy diffusivity for mass transfer, $ft^2/\text{hr}$
$\epsilon_{Moe}$	vertical eddy diffusivity for momentum transfer, $ft^2/\text{hr}$
$\epsilon_0, \epsilon_1, \epsilon_n$	coefficients in equations (52), (55), and (56)
$\theta$	time, hrs.
$\theta_0$	period of the sinusoidal boundary temperature and diffusivity waves, hrs.
$\lambda$	a variable defined by equation (16), $ft^2$
$\lambda'$	a variable of integration in equation (22)
$\Lambda(\lambda)$	a function of $\lambda$ defined in equation (23)
$\mu$	absolute air viscosity, $\# \text{hr}/ft^2$
$\nu$	constant in equation (24), $1/ft^2$
$\nu_n$	coefficients in equation (25), $1/ft^2$
$\nu'$	kinematic viscosity, $ft^2/\text{hr}$
$\rho$	mass density of fluid, $\# \text{hr}^2/ft^4$
$\sigma$	Stefan-Boltzmann constant, $17.3 \times 10^{-10} \text{ Btu}/ft^2(^{\circ}\text{R})^4$
$\tau$	fluid shear stress, $\#/ft^2$
$\tau_0$	fluid shear stress at the ground, $\#/ft^2$
$\phi_0$	amplitude of the complex function $H_0(1)$

$\omega$ 

frequency of the sinusoidal boundary temperature and diffusivity waves, radians/hr

Dimensionless Moduli:

$$Nu_r = \frac{E_0 z_r}{k}$$

$$Re_r = \frac{U_r z_r}{\nu}$$

$$Z^* = \frac{z \sqrt{T_0}}{\nu}$$

$$Pr = \frac{E \mu c_p}{k}$$

### INTRODUCTION

A number of transfer processes which are associated with current atmospheric diffusion problems are the diffusion of

- 1) air pollutants from industrial and other sources,
- 2) water vapor from lakes,
- 3) water vapor from snow banks,
- 4) heat and momentum from orchards, and
- 5) smokes and poisonous gases from grenades or bombs.

Each of these transfer processes falls into the general category of atmospheric diffusion.

The diffusion of heat, mass, and momentum in the atmosphere is achieved by a complicated turbulence mechanism which at present does not appear to be thoroughly understood. An exact fundamental relation describing eddy diffusion has not yet been determined. Several approximate eddy diffusion relations are available, however. One of the most useful of these approximate diffusion relations is the one which relates the rate of transfer of a quantity to a potential gradient and an eddy diffusivity.

The eddy diffusion rate of heat, mass, or momentum at the earth's surface, in particular, may be expressed in terms of flow potential differences and corresponding transfer conductances and coefficients. For example, vertical convective heat transfer rates at the earth's surface can be expressed in terms of air temperature differences and unit thermal convective conductances, and vertical momentum transfer rates at the earth's surface can be expressed in terms of wind velocities and drag coefficients.

If quantitative atmospheric turbulence data such as eddy diffusivity profiles, unit convective conductances, or drag coefficients are available, it is possible to estimate heat, mass, and momentum transfer rates or flow potential concentrations in the atmosphere for point source, line source, or

area source diffusion systems. These basic turbulent diffusion data must be available before satisfactory solutions to some of the current atmospheric diffusion problems can be effected.

The following paragraphs consist of a discussion of

- 1) some of the basic eddy diffusion relations to be considered,
- 2) some experimental methods of determining eddy diffusivities, thermal conductances, and drag coefficients,
- 3) analytical and numerical eddy diffusion analyses, and
- 4) the analysis of several sets of micrometeorological measurements by the methods outlined in this paper.

BASIC EDDY DIFFUSION RELATIONS

The eddy transfer rate of a quantity in the absence of atmospheric thermals is often expressed in terms of an eddy diffusivity and a potential gradient. For example, the vertical rate of convective heat transfer is, (Reference 1)

$$\left(\frac{q}{A}\right)_{conv} = -\gamma c_p \epsilon_{sH} \left(\frac{\partial T}{\partial z} + \Gamma\right) \quad (1)$$

where,

- $\gamma$  = air density
- $c_p$  = air heat capacity
- $\epsilon_{sH}$  = vertical thermal eddy diffusivity
- $T$  = mean air temperature
- $\Gamma$  = adiabatic lapse rate

Similarly, the vertical rate of momentum transfer in the absence of atmospheric thermals expressed in terms of the fluid shear stress is, (Reference 2)

$$\tau = \rho \epsilon_{sMoz} \left(\frac{\partial U}{\partial z}\right) \quad (2)$$

where,

- $\rho$  = mass density of air
- $\epsilon_{sMoz}$  = momentum eddy diffusivity in the z direction
- $U$  = mean air velocity

A mass transfer equation similar to equations (1) and (2) can also be written.

If a heat balance and a force balance are made on a differential lattice in a turbulent flow system, the transient eddy diffusion equations for heat and momentum transfer can be derived, respectively. For example, the heat transfer diffusion equation, when the molecular conduction terms are small, is, (Reference 3)

$$\frac{\partial T}{\partial \theta} + u \frac{\partial T}{\partial x} + v \frac{\partial T}{\partial y} + w \frac{\partial T}{\partial z} = \frac{\partial}{\partial x} \left( \epsilon_{sH} \frac{\partial T}{\partial x} \right) + \frac{\partial}{\partial y} \left( \epsilon_{sH} \frac{\partial T}{\partial y} \right) + \frac{\partial}{\partial z} \left( \epsilon_{sH} \frac{\partial T}{\partial z} \right) \quad (3)$$

where,

$\theta$  = time

$U, V, W$  = mean fluid velocities in  $x, y,$  and  $z$  directions, respectively

$\epsilon_{x'}, \epsilon_{y'}, \epsilon_{z'}$  = thermal eddy diffusivities in  $x, y,$  and  $z$  directions, respectively

The Navier-Stokes equations which were modified by Osborne Reynolds to include the fluctuating velocity components are similar to the heat transfer diffusion equation given above except for the presence of a pressure gradient term in each of the three hydrodynamic equations (Reference 4).

Sometimes it is convenient to express vertical heat and momentum transfer rates at the earth's surface (the boundary equations) in terms of flow potential differences and corresponding transfer conductances and coefficients rather than flow potential gradients and eddy diffusivities. This procedure has long been used in the field of engineering in connection with fluid flow and heat transfer systems of finite dimensions. The vertical rate of convective heat transfer at the earth's surface can be expressed as

$$\left(\frac{q}{A}\right)_{conv_0} = f_0 (T_s - T_r) \quad (4)$$

where,

$f_0$  = unit thermal convective conductance

$T_s$  = mean air-earth interface temperature

$T_r$  = mean air temperature at a reference height.

The shear stress can be expressed as

$$\tau_0 = \frac{1}{2} \rho C_D U_r^2 \quad (5)$$

where,

$C_D$  = drag coefficient

$U_r$  = mean air velocity at a reference height

The basic eddy diffusion relations that have been noted above are required for the diffusion analyses which are presented in the remainder of this paper.



EXPERIMENTAL TECHNIQUES OF DETERMINING  
EDDY DIFFUSIVITIES, THERMAL CONDUCTANCES, AND DRAG COEFFICIENTS

A. Vertical Convective Heat Transfer.

Because of the recent development of two simple thermal instruments, it is possible to measure vertical eddy diffusivity profiles and unit thermal conductances. A heat flow meter (References 5 and 6) has been developed at the University of California which can be used to measure heat flow rates into or out of the earth's surface. This heat flow meter consists of laminated sheets of thin bakelite with an embedded thermopile. Heat flow through this meter is measured in terms of the voltage response of the calibrated thermopile. A total hemispherical radiometer (Reference 7), also developed at the University of California, can be employed to measure the total solar and nocturnal irradiation upon the earth's surface as well as the radiosity of the earth's surface. Briefly, this instrument consists of a horizontal heat meter whose upper surface is blackened and whose lower surface is surfaced with a sheet of aluminum. Both the upper and lower surfaces of the heat meter are exposed to air streams of equal velocity originating from a small blower. If a complete heat rate balance is made on this system, it can be shown that the total hemispherical radiation falling upon the horizontal heat meter surface is equal to a constant times the voltage drop across the heat meter thermopile plus a datum term.

If a heat balance is made at the earth's surface, the convective plus evaporative heat transfer rates may be expressed as<sup>1</sup>

$$\left(\frac{q}{A}\right)_{conv_0} + \left(\frac{q}{A}\right)_{e_0} = \left(\frac{q}{A}\right)_{t.h._0} - \left(\frac{q}{A}\right)_{s.r.} + \left(\frac{q}{A}\right)_{s_0} \quad (6)$$

where,

$$\left(\frac{q}{A}\right)_{conv_0} = \text{convective heat transfer rate per unit area at the ground}$$

<sup>1</sup>The signs of the terms  $\left(\frac{q}{A}\right)_{conv_0}$ ,  $\left(\frac{q}{A}\right)_{e_0}$  and  $\left(\frac{q}{A}\right)_{s_0}$  depend upon solar radiation, air temperature, and vapor pressure increments.

- $\left(\frac{q}{\lambda}\right)_{t.h.0}$  - total hemispherical radiation per unit area at the ground  
 $\left(\frac{q}{\lambda}\right)_{g.r.}$  - ground radiosity per unit area  
 $\left(\frac{q}{\lambda}\right)_{s_0}$  - heat transfer rate per unit area into or out of the ground at the interface.  
 $\left(\frac{q}{\lambda}\right)_{e_0}$  - heat transfer rate per unit area due to evaporation or condensation of water vapor at the interface

In the absence of direct measurements of either the convective or latent heat transfer rates<sup>2</sup> the following method of separating the sum of these two terms is suggested. Equate the defining convective and latent heat transfer equations within the turbulent layer adjacent to the laminar sublayer to the sum under consideration.

$$\left(\frac{q}{\lambda}\right)_{conv_0} + \left(\frac{q}{\lambda}\right)_{e_0} = -\gamma c_p \epsilon_{s_H} \left(\frac{\partial T}{\partial z} + \Gamma\right) - l \epsilon_{Mass} \frac{\partial C}{\partial z} \quad (7)$$

where,

- $\epsilon_{Mass}$  - vertical eddy diffusivity for mass transfer  
 $\epsilon_{s_H}$  - vertical eddy diffusivity for heat transfer  
 $C$  - water vapor concentration  
 $l$  - latent heat of vaporisation

Several investigators in the literature have shown that the heat, mass, and momentum eddy diffusivities are closely related (References 9 and 10). It is thus proposed that the heat and mass transfer eddy diffusivities are related to each other by a constant,  $j$ . That is,

$$\frac{\epsilon_{Mass}}{\epsilon_{s_H}} = j \quad (8)$$

<sup>2</sup>Evaporimeters of the type used by Thornthwaite (Reference 8) would appear to be very useful in measuring mean evaporation rates if not instantaneous ones. Mass flow meters similar in principle to heat flow meters are currently being considered by the University of California, Los Angeles.

Upon the substitution of equation (8) into equation (7), the heat eddy diffusivity can be expressed as

$$\epsilon_{H} = \frac{\left(\frac{q}{A}\right)_{conv} + \left(\frac{q}{A}\right)_{e_0}}{\gamma c_p \left(\frac{\partial T}{\partial z} + \Gamma\right) + j l \left(\frac{\partial C'}{\partial z}\right)} \quad (9)$$

References 9 and 10 indicate that for duct flow systems, the constant,  $j$ , is equal to unity. Thus an approximate method of separating the convective and evaporative heat flow terms consists of postulating that the constant  $j = 1$ , solving for  $\epsilon_{H}$  by equation (9), and hence evaluating the convective and evaporative heat flow terms. The ratio,  $j$ , will become more firmly established with continuing micrometeorological research. In the event that one of the two heat flow terms is small compared to the other, no separation problem exists.

After having determined the convective heat transfer rate, it is possible to determine the convective heat transfer conductances and thermal eddy diffusivities from the defining basic eddy diffusion relations which have been presented previously. Mass transfer conductances and diffusivities may be obtained in a similar manner.

Some limited convective heat transfer measurements and calculated thermal conductances are presented in a following section.

#### B. Vertical Momentum Transfer

Boundary drag force measurements in pipe flow systems can be made with relative ease in comparison to boundary drag force measurements in the atmospheric system. No direct measurements of the drag force exerted by the wind on the earth's surface appear to be reported in the literature with the exception of those of P.A. Sheppard (Reference 11).

The problem of measuring the air shear stress at the earth's surface essentially consists of determining the drag force on a small area of that surface 1) whose surface characteristics are representative of the surrounding

surface and 2) which is so located that the velocity profile above it is typical of the surrounding velocity profile (no new boundary layers initiated). The atmospheric shear meter that was developed by the University of California was designed with the above two requisites in mind and has yielded encouraging results. This shear meter essentially consisted of a large tank filled with water into which was placed a shallow float whose surface was representative of the surroundings. Drag forces were measured by noting the deflection of a sensitive coil spring, one end of which was attached to the float and the other end to the rim of the tank. Abrupt flow discontinuities were avoided by filling the latter to within less than  $1/16$  of an inch of the brim with water and adjusting the weight of the float so that it extended less than  $1/16$  inch above the water surface. The tank rim, float surface, water surface, and surrounding earth surface were thereby essentially in one plane. Smoke flow studies indicated that smooth air flow conditions existed over the shear meter.

The shear meter construction details are shown in Figure 1. The tank was 48 inches in diameter and 3 inches deep; the respective dimensions of the float were 36 and  $2\frac{1}{4}$  inches. It was necessary to cover the upper float surface with a thin layer of earth in order to create a surface which was similar to the surroundings. The total weight of this float was about seventy-five pounds. Because it was desired to measure the mean shear stress rather than the instantaneous values, a coil spring with a very low spring constant was utilized in order that the shear fluctuations superposed upon the mean shear would not cause the float to oscillate. The coil spring was made by winding piano wire (0.007 inch diameter) on a steel rod. One end of the spring was attached to the rim of the tank by a clip which could be rotated when significant changes in wind direction occurred. The other end of the spring was fixed to a wire located under the float and attached to the float center. This arrangement allowed angular freedom of the float without producing spring extension due to angular

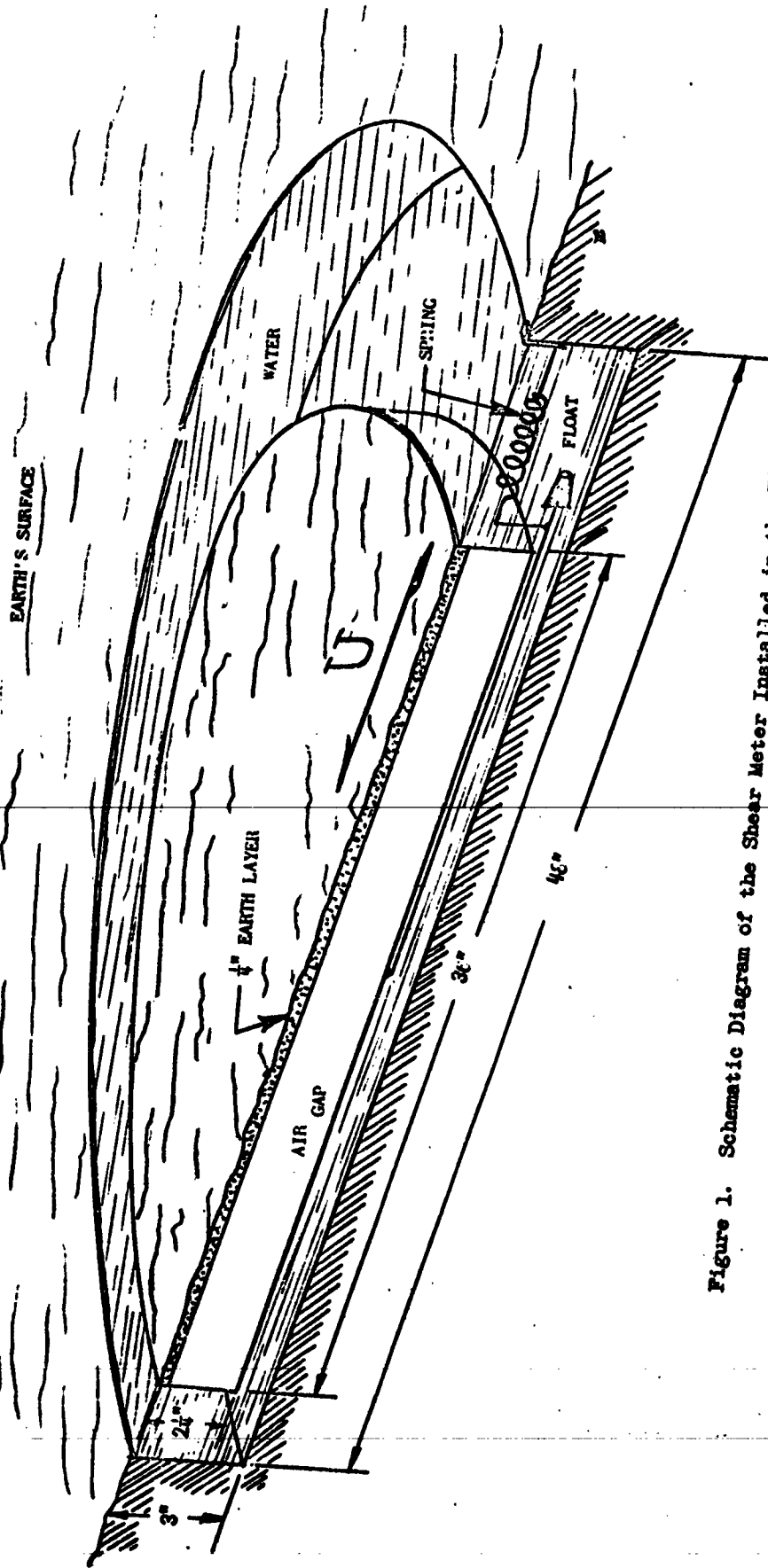


Figure 1. Schematic Diagram of the Shear Meter Installed in the Field

float rotation. The drag force for this simple spring system is given by

$$F_D = \tau_0 A_s = k_s \delta_s \quad (10)$$

where,

$k_s$  = spring constant

$\delta_s$  = deflection of the spring

$A_s$  = shear meter surface area exposed to air flow

The spring constant for the particular spring used was 0.001 lbs/inch and was accurate within one percent.

Although the shear meter that has been described was developed independently of Sheppard's meter, the two instruments are similar. However, Sheppard's meter was based on a torsion principle rather than a tension principle, and also his meter was designed to measure drag forces over smooth surfaces. Field experience with the authors' present shear meter has indicated that the following improvements are desirable: 1) a response system which is independent of wind direction and 2) a shear stress recording mechanism. Development of future instruments having these improvements has been initiated.

After having determined the shear stress with the aid of a shear meter, it is possible to calculate the drag coefficient and momentum eddy diffusivity from the defining eddy diffusion relations which have been presented previously.

Some limited shear stress measurements and calculated drag coefficients and eddy diffusivities are presented in a following section.

ANALYTICAL AND NUMERICAL EDDY DIFFUSION ANALYSES

## A. Analytical Analyses

A number of analytical eddy diffusion analyses can be found in the literature. Prandtl (Reference 12) derived the steady state logarithmic velocity profile for the surface layer.<sup>3</sup> Rossby and Montgomery (Reference 13) and Sverdrup (Reference 14) developed steady state wind velocity profiles for the surface layer for adiabatic and stable atmospheres. Lettau (Reference 15) has recently derived steady state velocity and temperature profile expressions for the surface layer for adiabatic and non-adiabatic atmospheres. O. G. Sutton (Reference 16) has developed point and line-source eddy diffusion solutions for stable atmospheres. Brunt (Reference 17) has presented a periodic convective heat flow solution for a system in which the boundary temperature varies sinusoidally with time, thus approximating the diurnal soil-air interface temperature variation; the eddy diffusivity was postulated to be independent of time and height. Haurwitz (Reference 18) has developed a periodic convective heat flow solution for a system in which the boundary temperature varies sinusoidally with time and the eddy diffusivity varies linearly with height but is independent of time.

In the following paragraphs, two new periodic convection analyses in the absence of atmospheric thermals are presented. One analysis pertains to an eddy diffusion system in which the boundary temperature varies sinusoidally with time and the eddy diffusivity varies sinusoidally with time (to approximate unstable diffusion during the day and stable diffusion at night.) Another analysis pertains to an eddy diffusion system in which the boundary temperature varies sinusoidally with time and the eddy diffusivity varies sinusoidally with time and linearly with height.

## 1) Eddy Diffusivity Varies Sinusoidally With Time But Not With Height

The heat transfer differential and boundary equations for the system under

---

<sup>3</sup>The surface layer has been defined as the air layer adjacent to the earth's surface where the vertical convective heat flow and vertical fluid shear stress are uniform with height.

consideration are<sup>4</sup>

$$\frac{\partial t}{\partial \theta} = \frac{\partial}{\partial z} \left( \epsilon_{zg} \frac{\partial t}{\partial z} \right) \quad (11)$$

$$t(0, \theta) = t_0 \cos \omega \theta \quad (12)$$

$$\lim_{z \rightarrow \infty} t(z, \theta) = 0 \quad (13)$$

where,

$$\epsilon_{zg} = c_1 + c_2 \cos \omega \theta \quad (14)$$

$t$  = potential temperature

$t_0$  = amplitude of the sinusoidal boundary temperature wave

$\omega$  = frequency of the sinusoidal boundary temperature and diffusivity waves

$\theta_0$  = period of the sinusoidal boundary temperature and diffusivity waves

$c_1, c_2$  = constants in equation(14)

If the differentiation indicated in equation (11) is performed, the following equation results:

$$\frac{1}{\epsilon_{zg}} \frac{\partial t}{\partial \theta} = \left( \frac{1}{c_1 + c_2 \cos \omega \theta} \right) \frac{\partial t}{\partial \theta} = \frac{\partial^2 t}{\partial z^2} \quad (15)$$

Equation(15) can be simplified by making a change of variable.

$$\text{Let} \quad \lambda = c_1 \theta + \frac{c_2}{\omega} \sin \omega \theta \quad (16)$$

$$\text{Then} \quad \frac{\partial \lambda}{\partial \theta} = c_1 + c_2 \cos \omega \theta \quad (17)$$

Now the left hand term of equation(15) can be simplified as follows:

$$\left( \frac{1}{c_1 + c_2 \cos \omega \theta} \right) \frac{\partial t}{\partial \theta} = \left( \frac{1}{c_1 + c_2 \cos \omega \theta} \right) \frac{\partial \lambda}{\partial \theta} \frac{\partial t}{\partial \lambda} = \frac{\partial t}{\partial \lambda} \quad (18)$$

<sup>4</sup>These equations are expressed in terms of the potential temperature rather than the ordinary temperature. Potential temperature can be expressed as  $t = T + \Gamma z$ .



The transformed differential and boundary equations are

$$\frac{\partial \tau}{\partial \lambda} = \frac{\partial^2 \tau}{\partial z^2} \quad (19)$$

$$\tau(0, \lambda) = \tau_0 \cos \omega f(\lambda) \quad (20)$$

$$\lim_{z \rightarrow \infty} \tau(z, \lambda) = 0 \quad (21)$$

where,  $f(\lambda) = \theta$

It can be shown that the function  $\tau(0, \lambda)$  is an even periodic function with a period  $c_1 \theta_0$  where  $\theta_0$  is the period of the sinusoidal boundary temperature and diffusivity variations. The function  $\tau(0, \lambda)$  may thus be expressed as the Fourier cosine series

$$\tau(0, \lambda) = \frac{a_0}{2} + \sum_{n=1}^{\infty} a_n \cos \frac{2n\pi\lambda}{c_1\theta_0} \quad (22)$$

where,

$$a_0 = \frac{4}{c_1\theta_0} \int_0^{\frac{c_1\theta_0}{2}} \tau(\lambda') d\lambda'$$

$$a_n = \frac{4}{c_1\theta_0} \int_0^{\frac{c_1\theta_0}{2}} \tau(\lambda') \cos \frac{2n\pi\lambda'}{c_1\theta_0} d\lambda'$$

Equation (19) can be solved by the separation of variables technique.

$$\text{Let } \tau = Z(z)\Lambda(\lambda) \quad (23)$$

where  $Z(z)$  and  $\Lambda(\lambda)$  are functions of  $z$  and  $\lambda$ , respectively. The steady state periodic solution of equation (23) which satisfies equations (20) and (21) is

$$Z(z) = \text{constant}_1 e^{-\sqrt{\nu}z}, \quad \Lambda(\lambda) = \text{constant}_2 e^{i\nu\lambda}$$

$$\text{or } \tau = C e^{-\sqrt{\nu}z} e^{i\nu\lambda} = C e^{\frac{\sqrt{\nu}}{2}z} e^{i\left(-\frac{\sqrt{\nu}}{2}z + \nu\lambda\right)} \quad (24)$$

The transformed differential and boundary equations are

$$\frac{\partial t}{\partial \lambda} = \frac{\partial^2 t}{\partial z^2} \quad (19)$$

$$t(0, \lambda) = t_0 \cos \omega f(\lambda) \quad (20)$$

$$\lim_{z \rightarrow \infty} t(z, \lambda) = 0 \quad (21)$$

where,  $f(\lambda) = \theta$

It can be shown that the function  $t(0, \lambda)$  is an even periodic function with a period  $c_1 \theta_0$  where  $\theta_0$  is the period of the sinusoidal boundary temperature and diffusivity variations. The function  $t(0, \lambda)$  may thus be expressed as the Fourier cosine series

$$t(0, \lambda) = \frac{a_0}{2} + \sum_{n=1}^{\infty} a_n \cos \frac{2n\pi\lambda}{c_1\theta_0} \quad (22)$$

where,

$$a_0 = \frac{4}{c_1\theta_0} \int_0^{c_1\theta_0/2} t(\lambda') d\lambda'$$

$$a_n = \frac{4}{c_1\theta_0} \int_0^{c_1\theta_0/2} t(\lambda') \cos \frac{2n\pi\lambda'}{c_1\theta_0} d\lambda'$$

Equation (19) can be solved by the separation of variables technique.

$$\text{Let } t = Z(z)\Lambda(\lambda) \quad (23)$$

where  $Z(z)$  and  $\Lambda(\lambda)$  are functions of  $z$  and  $\lambda$ , respectively. The steady state periodic solution of equation (23) which satisfies equations (20) and (21) is

$$Z(z) = \text{constant}_1 e^{-\sqrt{\nu}z}, \quad \Lambda(\lambda) = \text{constant}_2 e^{i\nu\lambda}$$

$$\text{or } t = C_0 e^{-\sqrt{\nu}z} e^{i\nu\lambda} = C_0 e^{-\sqrt{\nu}z} e^{i(\sqrt{\nu}z + \nu\lambda)} \quad (24)$$

where,  $C$  and  $\nu$  are constants which are to be determined and  $i = \sqrt{-1}$ . Both the real and imaginary parts of the complex solution given in equation (24) are solutions of the original differential equation. On physical grounds, the real part of equation (24) must be chosen. Also, the solution must be expressed in terms of a series because this is the form of the boundary equation (22).

$$\text{Thus, } t(z, \lambda) = \sum_{n=0}^{\infty} C_n \cdot \sqrt{\frac{\nu_n}{2}} z \cos\left(\nu_n \lambda - \sqrt{\frac{\nu_n}{2}} z\right) \quad (25)$$

when  $n = 0, 1, 2, \dots$

The constants  $C_n$  and  $\nu_n$  are determined from the boundary equation (22).

At  $z = 0$ ,

$$t(0, \lambda) = \frac{a_0}{2} + \sum_{n=1}^{\infty} a_n \cos \frac{2n\pi\lambda}{c_1 \theta_0} = C_0 + \sum_{n=1}^{\infty} C_n \cos \nu_n \lambda$$

Thus,

$$C_0 = \frac{a_0}{2}$$

$$C_n = a_n \text{ for } n = 1, 2, \dots \quad (26)$$

$$\nu_n = \frac{2n\pi}{c_1 \theta_0}$$

The temperature solution for the heat transfer system under consideration is

$$T(z, \theta) = T_s + \sum_{n=0}^{\infty} C_n \cdot \sqrt{\frac{\nu_n}{2}} z \cos\left(\frac{2n\pi\theta}{\theta_0} + \frac{n c_2}{c_1} \sin \frac{2\pi\theta}{\theta_0} - \sqrt{\frac{\nu_n}{2}} z\right) \quad (27)$$

where,  $n = 0, 1, 2, \dots$

and

$$C_0 = \frac{2}{c_1 \theta_0} \int_0^{\theta_0} t(\lambda) d\lambda$$

and,

$$C_h = \frac{4}{c_1 \theta_0} \int_0^{\frac{c_1 \theta_0}{2}} t(\lambda') \cos \frac{2n\pi\lambda'}{c_1 \theta_0} d\lambda'$$

The periodic vertical heat flow solution for the heat transfer system under consideration can be obtained by substituting the temperature solution given in equation (27) into equation (1)

$$\left(\frac{q}{A}\right)_{conv} = -\gamma c_p \epsilon_{sH} \left(\frac{\partial T}{\partial z} + \Gamma\right) \quad (1)$$

Mass concentration and mass flow rate solutions can be derived just as the temperature and heat flow solutions were derived above if the mass transfer system possesses the above stipulated boundary and eddy diffusivity equations.

## 2) Eddy Diffusivity Varies Sinusoidally With Time and Linearly With Height

The heat transfer differential and boundary equations under consideration are

$$\frac{\partial c}{\partial \theta} = \frac{\partial}{\partial z} \left( \epsilon_{sH} \frac{\partial c}{\partial z} \right) \quad (28)$$

$$c(0, \theta) = c_0 \cos \omega \theta \quad (29)$$

$$\lim_{z \rightarrow \infty} c(z, \theta) = 0 \quad (30)$$

where,

$$\epsilon_{sH} = (b_1 + b_2 z) (1 + b_3 \cos \omega \theta) \quad (31)$$

$b_1$ ,  $b_2$ , and  $b_3$  are constants in equation (31)

If the differentiation indicated in equation (28) is performed, there results

the following equation

$$\begin{aligned} \frac{\partial t}{\partial \theta} &= \frac{\partial \epsilon_{s1}}{\partial z} \frac{\partial t}{\partial z} + \epsilon_{s1} \frac{\partial^2 t}{\partial z^2} \\ &= (1 + b_2 \cos \omega \theta) b_2 \frac{\partial t}{\partial z} + (b_1 + b_2 z) (1 + b_2 \cos \omega \theta) \frac{\partial^2 t}{\partial z^2} \end{aligned}$$

or

$$\left( \frac{1}{1 + b_2 \cos \omega \theta} \right) \frac{\partial t}{\partial \theta} = b_2 \frac{\partial t}{\partial z} + (b_1 + b_2 z) \frac{\partial^2 t}{\partial z^2} \quad (32)$$

Equation (32) can be simplified by making a change of variable.

$$\text{Let} \quad \beta = \theta + \frac{b_2}{\omega} \sin \omega \theta \quad (33)$$

$$\text{Then} \quad \frac{\partial \beta}{\partial \theta} = 1 + b_2 \cos \omega \theta \quad (34)$$

The left hand term of equation (32) can be simplified as follows:

$$\left( \frac{1}{1 + b_2 \cos \omega \theta} \right) \frac{\partial t}{\partial \theta} = \left( \frac{1}{1 + b_2 \cos \omega \theta} \right) \frac{\partial \beta}{\partial \theta} \frac{\partial t}{\partial \beta} = \frac{\partial t}{\partial \beta} \quad (35)$$

The transformed differential and boundary equations are

$$\frac{\partial t}{\partial \beta} = b_2 \frac{\partial t}{\partial z} + (b_1 + b_2 z) \frac{\partial^2 t}{\partial z^2} \quad (36)$$

$$t(0, \beta) = t_0 \cos \omega f(\beta) \quad (37)$$

$$\lim_{z \rightarrow \infty} t(z, \beta) = 0 \quad (38)$$

where,  $f(\beta) = \theta$

The function  $t(0, \beta)$  is an even periodic function with a period  $\theta_0$  and thus may be expressed as a Fourier cosine series,

$$t(0, \beta) = \frac{t_0}{2} + \sum_{n=1}^{\infty} E_n \cos \frac{2n\pi\beta}{\theta_0} \quad (39)$$

where,

$$\epsilon_0 = \frac{4}{\theta_0} \int_0^{\theta_0} \frac{1}{2} \epsilon(\beta) a \beta$$

$$\epsilon_n = \frac{4}{\theta_0} \int_0^{\theta_0} \frac{1}{2} \epsilon(\beta) \cos \frac{2n\pi\beta}{\theta_0} a \beta$$

A further change of variable will simplify the differential equation (36).

$$\text{Let } r^2 = b_1 + b_2 z \quad (40)$$

Then equation (36) reduces to

$$\frac{\partial \epsilon}{\partial \beta} = \frac{b_2^2}{4} \frac{\partial^2 \epsilon}{\partial r^2} + \frac{b_2^2}{4r} \frac{\partial \epsilon}{\partial r} \quad (41)$$

Equation (41) can be solved by the separation of variables technique.

$$\text{Let } \epsilon = R(r) B(\beta) \quad (42)$$

where  $R(r)$  and  $B(\beta)$  are functions of  $r$  and  $\beta$ , respectively. The steady state periodic solution of equation (41) which satisfies equations (37) and (38) is

$$R(r) = \text{constant}_1 H_0^{(1)} \left( \frac{2\sqrt{P}}{b_2} \sqrt{i} r \right), \quad B(\beta) = \text{constant}_2 e^{-iP\beta}$$

$$\text{or } \epsilon = E e^{-iP\beta} H_0^{(1)} \left( \frac{2\sqrt{P}}{b_2} \sqrt{i} r \right) \quad (43)$$

where  $E$  and  $P$  are constants to be determined and where the function

$$H_0^{(1)} \left( \frac{2\sqrt{P}}{b_2} \sqrt{i} r \right) \text{ can be expressed as } \frac{2}{\pi} \left[ \text{ker} \left( \frac{2\sqrt{P}}{b_2} r \right) + i \text{ker} \left( \frac{2\sqrt{P}}{b_2} r \right) \right] \text{ or } M_0 \left( \frac{2\sqrt{P}}{b_2} r \right) e^{i\phi_0 \left( \frac{2\sqrt{P}}{b_2} r \right)}$$

(Reference 19). The term  $M_0 \left( \frac{2\sqrt{P}}{b_2} r \right)$  is the modulus and the term  $\phi_0 \left( \frac{2\sqrt{P}}{b_2} r \right)$  the

amplitude of the complex function  $H_0^{(1)} \left( \frac{2\sqrt{P}}{b_2} \sqrt{i} r \right)$ .

That is,

$$M_0 \left( \frac{2\sqrt{p}}{b_2} r \right) = \frac{2}{\pi} \sqrt{\left( \operatorname{ker} \left( \frac{2\sqrt{p}}{b_2} r \right) \right)^2 + \left( \operatorname{ker} \left( \frac{2\sqrt{p}}{b_2} r \right) \right)^2} \quad (44)$$

and

$$\tan \phi_0 \left( \frac{2\sqrt{p}}{b_2} r \right) = \frac{\operatorname{ker} \left( \frac{2\sqrt{p}}{b_2} r \right)}{\operatorname{ker} \left( \frac{2\sqrt{p}}{b_2} r \right)} \quad (45)$$

Thus equation (43) may be expressed as

$$\begin{aligned} \tau &= E e^{-ip\beta} M_0 \left( \frac{2\sqrt{p}}{b_2} \sqrt{b_1 + b_2 z} \right) e^{i\phi_0 \left( \frac{2\sqrt{p}}{b_2} \sqrt{b_1 + b_2 z} \right)} \\ &= E M_0 \left( \frac{2\sqrt{p}}{b_2} \sqrt{b_1 + b_2 z} \right) e^{i \left( -p\beta + \phi_0 \left( \frac{2\sqrt{p}}{b_2} \sqrt{b_1 + b_2 z} \right) \right)} \end{aligned} \quad (46)$$

The constant E must be equal to  $\frac{E_0}{M_0 \left( \frac{2\sqrt{p}}{b_2} \sqrt{b_1} \right) e^{i\phi_0 \left( \frac{2\sqrt{p}}{b_2} \sqrt{b_1} \right)}}$

in order that the boundary condition can be satisfied, that is  $\tau(z=0)$  must

be of the form  $e^{-ip\beta}$  (the real part being  $\cos p\beta$ ).

$$\text{Thus, } \tau = \frac{E_0 M_0 \left( \frac{2\sqrt{p}}{b_2} \sqrt{b_1 + b_2 z} \right) e^{i \left( \phi_0 \left( \frac{2\sqrt{p}}{b_2} \sqrt{b_1 + b_2 z} \right) - \phi_0 \left( \frac{2\sqrt{p}}{b_2} \sqrt{b_1} \right) - p\beta \right)}}{M_0 \left( \frac{2\sqrt{p}}{b_2} \sqrt{b_1} \right)} \quad (47)$$

where,  $E_0$  is a constant

The real part of solution (47) is chosen on physical grounds. Also, the solution must be expressed in terms of a series as is the boundary equation.

Thus,

$$\tau(z, \beta) = \sum_{n=0}^{\infty} e_n \frac{M_0 \left( \frac{2\sqrt{p_n}}{b_2} \sqrt{b_1 + b_2 z} \right)}{M_0 \left( \frac{2\sqrt{p_n}}{b_2} \sqrt{b_1} \right)} \cos \left( \phi_0 \left( \frac{2\sqrt{p_n}}{b_2} \sqrt{b_1 + b_2 z} \right) - \phi_0 \left( \frac{2\sqrt{p_n}}{b_2} \sqrt{b_1} \right) - p_n \beta \right) \quad (48)$$

The constants  $e_n$  and  $p_n$  are determined from the boundary equation.

$$\text{At } z = 0, \quad t(0, \beta) = \frac{\xi_0}{2} + \sum_{n=1}^{\infty} \xi_n \cos \frac{2n\pi\beta}{\theta_0} = e_0 + \sum_{n=1}^{\infty} e_n \cos p_n \beta \quad (49)$$

Thus,

$$e_0 = \frac{\xi_0}{2}$$

$$e_n = \xi_n \quad \text{for } n = 1, 2, \dots$$

$$p_n = \frac{2n\pi}{\theta_0} \quad \text{for } n = 1, 2, \dots$$

Thus, the temperature solution for the heat transfer system under consideration

is

$$T(z, \theta) = Tz + e_0 + \sum_{n=1}^{\infty} e_n \frac{\sqrt{\left[ \ker \left( \frac{2\sqrt{p_n}}{b_2} \sqrt{b_1 + b_2 z} \right)^2 + \left[ \ker \left( \frac{2\sqrt{p_n}}{b_2} \sqrt{b_1 + b_2 z} \right) \right]^2} \cos \left( \frac{2n\pi\beta - \pi}{\theta_0} \right)}{\sqrt{\left[ \ker \left( \frac{2\sqrt{p_n}}{b_2} \sqrt{b_1} \right) \right]^2 + \left[ \ker \left( \frac{2\sqrt{p_n}}{b_2} \sqrt{b_1} \right) \right]^2}}$$

where,

$$n = 1, 2, 3, \dots$$

$$e_0 = \frac{2}{\theta_0} \int_0^{\frac{\theta_0}{2}} t(\beta) d\beta$$

$$e_n = \frac{4}{\theta_0} \int_0^{\frac{\theta_0}{2}} t(\beta) \cos \frac{2n\pi\beta}{\theta_0} d\beta \quad \text{for } n = 1, 2, \dots$$

$$\tan \pi = \frac{\ker \left( \frac{2\sqrt{p_n}}{b_2} \sqrt{b_1 + b_2 z} \right) \ker \left( \frac{2\sqrt{p_n}}{b_2} \sqrt{b_1} \right) - \ker \left( \frac{2\sqrt{p_n}}{b_2} \sqrt{b_1} \right) \ker \left( \frac{2\sqrt{p_n}}{b_2} \sqrt{b_1 + b_2 z} \right)}{\ker \left( \frac{2\sqrt{p_n}}{b_2} \sqrt{b_1 + b_2 z} \right) \ker \left( \frac{2\sqrt{p_n}}{b_2} \sqrt{b_1} \right) + \ker \left( \frac{2\sqrt{p_n}}{b_2} \sqrt{b_1 + b_2 z} \right) \ker \left( \frac{2\sqrt{p_n}}{b_2} \sqrt{b_1} \right)}$$

$$\beta = \theta + \frac{b_2}{\omega} \sin \omega \theta$$

(50)



### B. Numerical Analyses

Several numerical methods of evaluating eddy diffusivity profiles from transient air temperature and humidity profiles in the atmosphere have been given in the literature (References 20 and 21, for example). These methods usually involve replacing the differential equation describing transient diffusion by a finite difference equation. When experimental temperature or humidity data are substituted into the finite difference equation, a solution can be effected. Some of these methods involve procedures which do not appear to be sufficiently general. For example, one method requires that at one time in the analysis, eddy diffusivities in adjacent air layers be the same. Another method requires an error analysis to be applied to the resulting diffusivity data because of an over simplified postulate that was used; this error analysis then invalidates much of the data.

Three numerical methods of determining eddy diffusivities as a function of height and time from transient temperature and humidity profiles are presented below. These methods, which do not appear to be presented in the literature, possess several desirable advantages.

#### Method No. 1

A heat rate balance on a volume of air  $z_2 - z_1$  units thick with a unit area base is

$$\gamma_2 c_p \epsilon_2 \left( \frac{\partial T}{\partial z} + \Gamma \right)_2 - \gamma_1 c_p \epsilon_1 \left( \frac{\partial T}{\partial z} + \Gamma \right)_1 = \int_{z_1}^{z_2} \gamma c_p \frac{\partial T}{\partial \theta} dz \quad (51)$$

It is now postulated that the eddy diffusivity varies linearly with height, that is

$$\epsilon = \epsilon_0 + \epsilon_1 z \quad (52)$$

where  $\epsilon_0$  and  $\epsilon_1$  are constants for a given time. If it is desired to determine the eddy diffusivity profile (a linear one which approximates the actual one) in a given air layer, the following procedure is suggested. Divide the layer in question into two layers and write equation (51) for each of them. Upon substituting the

linear diffusivity relation given by equation (52) into the two heat balance equations, there result the following two equations:

$$\gamma_2 c_{p_2} (\epsilon_0 + \epsilon_1 z_2) \left( \frac{\partial T}{\partial z} + \Gamma \right)_2 - \gamma_1 c_{p_1} (\epsilon_0 + \epsilon_1 z_1) \left( \frac{\partial T}{\partial z} + \Gamma \right)_1 = \int_{z_1}^{z_2} \gamma c_p \frac{\partial T}{\partial \theta} dz \quad (53)$$

$$\gamma_2 c_{p_2} (\epsilon_0 + \epsilon_1 z_2) \left( \frac{\partial T}{\partial z} + \Gamma \right)_2 - \gamma_2 c_{p_2} (\epsilon_0 + \epsilon_1 z_2) \left( \frac{\partial T}{\partial z} + \Gamma \right)_2 = \int_{z_2}^{z_2} \gamma c_p \frac{\partial T}{\partial \theta} dz \quad (54)$$

If density, heat capacity, adiabatic lapse rate, and temperature gradient data for a given set of experimental temperature measurements at a given time are substituted into equations (53) and (54), and if the integrations indicated are performed, there result two algebraic equations in two unknowns ( $\epsilon_0$  and  $\epsilon_1$ ). The solutions of these equations are easily obtained.

#### Method No. 2

A somewhat more general eddy diffusivity distribution can be expressed by the following power expression:

$$\epsilon = \epsilon_0 z^{\epsilon_1} \quad (55)$$

where  $\epsilon_0$  and  $\epsilon_1$  are constants for a given time. Upon substituting equation (55) into the two heat balance equations and inserting the experimental property and temperature data, as was indicated in Method No. 1 above, two solvable algebraic equations in two unknowns result.

#### Method No. 3

An eddy diffusivity distribution which is very general is the following series containing 'n' terms:

$$\epsilon = \epsilon_0 + \epsilon_1 z + \epsilon_2 z^2 + \dots + \epsilon_{n-1} z^{n-1} \quad (56)$$

where  $\epsilon_0, \epsilon_1, \dots, \epsilon_{n-1}$  are constants for a given time. Upon dividing the air layer under consideration into 'n' smaller layers and substituting equation

(56) into the 'n' heat balance equations, there would result 'n' algebraic equations in 'n' unknowns. If 'n' is a large number, these equations could be solved with the aid of computing machines.

Methods 1, 2, and 3 are thus suggested as rapid techniques of determining transient eddy diffusivity profiles for heat and mass transfer from transient temperature and moisture data. These methods are founded on general postulates.

ANALYSIS OF SEVERAL SETS OF MICROMETEOROLOGICAL DATA

A. Experimental Determination of Convective Heat Flows, Convective Conductances, Shear Stresses, Drag Coefficients, and Eddy Diffusivities.

1. Heat Transfer

On a clear summer day between the hours of 10:00 A.M. and 3:00 P.M. on August 12, 1949, a preliminary air-earth interface heat balance study was conducted near Van Nuys, California (Reference 22). This study involved the measurement of 1) air temperature profiles in the lower four feet, 2) earth temperature profiles in the upper ten inches, 3) solar irradiation, 4) ground heat flows, and 5) wind velocities at a five foot height. The experimental site was located on a large flat field covered with scattered, short brush less than a foot high. Thermocouples, a directional radiometer (Reference 23), a heat meter, and a cup anemometer were used to measure the temperature, radiation, ground heat flow, and wind velocity, respectively.

The interface heat balance relation, equation (6), may be expressed as

$$\left(\frac{q}{\lambda}\right)_{conv_0} + \left(\frac{\eta}{\lambda}\right)_{e_0} = \alpha_g \left(\frac{q}{\lambda}\right)_{solar} + \alpha_g \left(\frac{q}{\lambda}\right)_{gaseous} - \alpha_g \sigma T_s^4 + \left(\frac{q}{\lambda}\right)_{e_0} \quad (57)$$

The total hemispherical radiation and ground radiosity have been expressed in terms of solar, gaseous, and ground radiation<sup>5</sup>. The symbols  $\alpha_g$ ,  $\sigma$  and  $T_s$  are the grey-body earth surface emissivity, Stefan-Boltzmann constant, and the interface temperature, respectively. Because the ground was dry and had not been exposed to rain for more than a two month period the evaporative heat loss term  $\left(\frac{q}{\lambda}\right)_{e_0}$  was postulated to be small compared to the other terms in the equation. The solar radiation and ground heat flow terms were measured by the instruments described above. Data in the literature and some recent measurements by the Thermal Radiation Project at the University of California indicated that  $\alpha_g$  was very close to 0.8. The

term  $\left[ \alpha_g \left(\frac{q}{\lambda}\right)_{gaseous} - \alpha_g \sigma T_s^4 \right]$  was estimated from nocturnal (gaseous)

<sup>5</sup>Had a hemispherical radiometer rather than a directional radiometer been available at the experimental site, this re-arrangement of equation (6) would not have been necessary.

radiation calculations (Reference 24) and the interface temperature measurements. This estimate was in agreement with measurements by Brooks and Kelly (Reference 25). It was thus possible to calculate the convective heat loss using equation (57).

The results of the Van Nuys heat transfer study are presented in Figures 2, 3, 4, and 5. The unit thermal conductance, calculated by equation (4) and shown in Figure 2, is observed to be approximately proportional to the wind velocity (Figure 3). It is interesting to recall that the thermal conductance for turbulent flow in ducts and over flat plates varies as the eight tenths power of the fluid velocity. The magnitude of the thermal conductances were in agreement with certain measurements by F. A. Brooks (Reference 25), which were made under similar circumstances. Figure 4 reveals the variation of air temperature difference between the surface and four feet with time. Figure 5 shows the vertical convective heat flow which appears to have a maximum near one o'clock; this maximum almost coincides with the solar irradiation maximum (at 12:30 P.M.) and the surface-air temperature increment maximum (at 12:30 P.M.).

## 2. Momentum Transfer

Preliminary momentum transfer studies in the lower twenty feet of the atmosphere were conducted at intervals during January and February, 1950, at Riverside, California. These studies involved the measurement of wind velocity profiles and atmospheric shear stresses. Sensitive cup anemometers and the shear meter, which has previously been described, were used to measure wind velocity and shear stress, respectively. The experimental site was located on a flat rectangular field which had a disked surface, settled and flattened by rain. The few rough portions of ground that did exist within ten to twenty feet of the shear meter were smoothed with a rake. No vegetation covered this field, although some scattered patches of grass were noted on the last day of operation (February 20th). Most of the experimental measurements were made in the afternoon, between 2:00 and 4:30; atmospheric conditions of slight instability existed at these times. A few measurements were

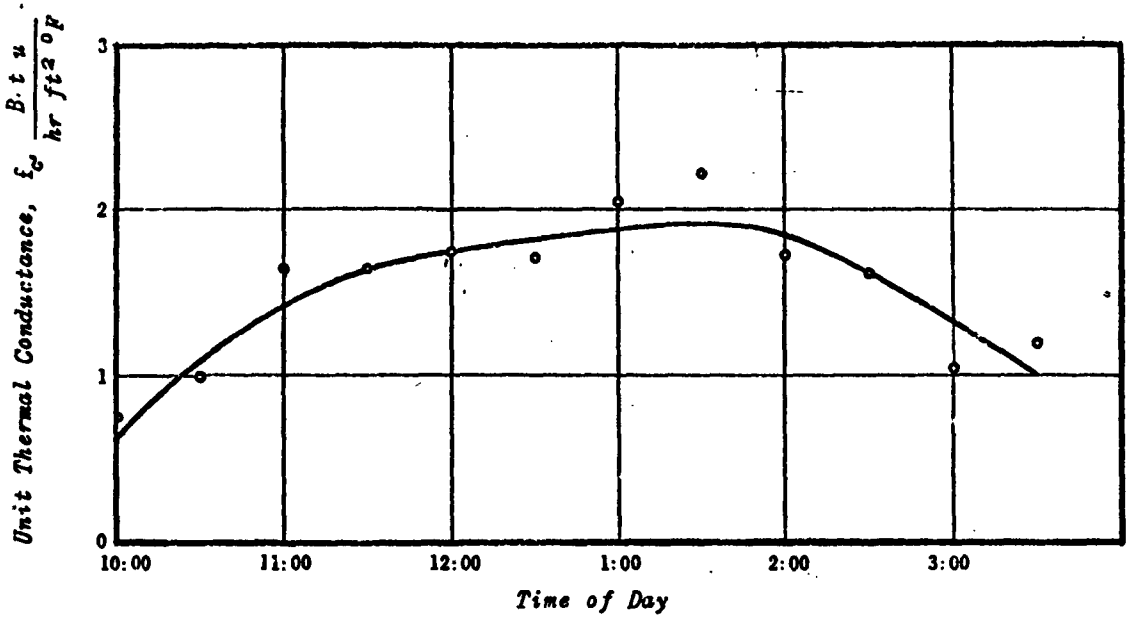


Figure 2. Unit Thermal Conductance for the Earth's Surface Versus Time

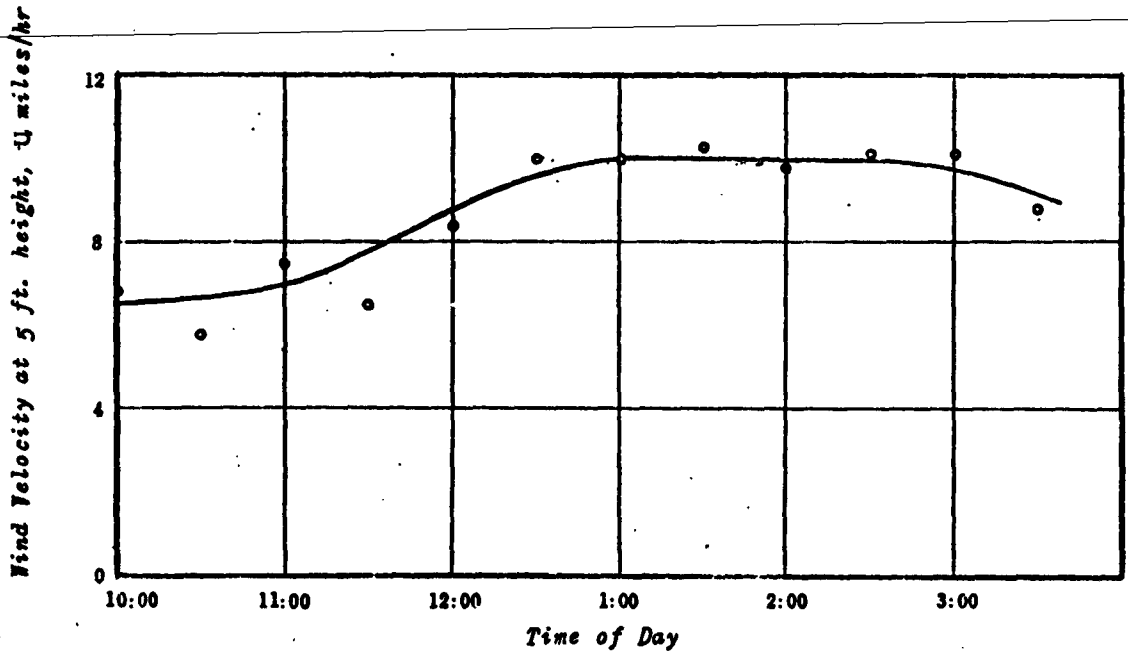


Figure 3. Wind Velocity as a Function of Time

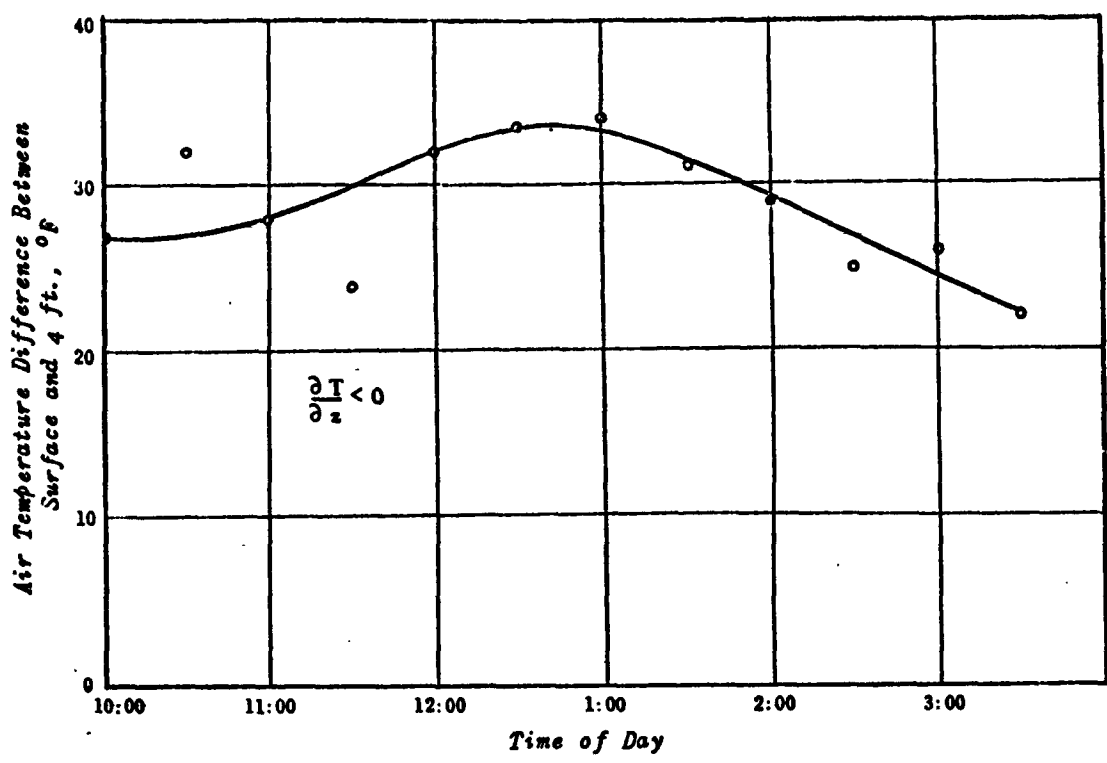


Figure 4. Air Temperature Difference as a Function of Time

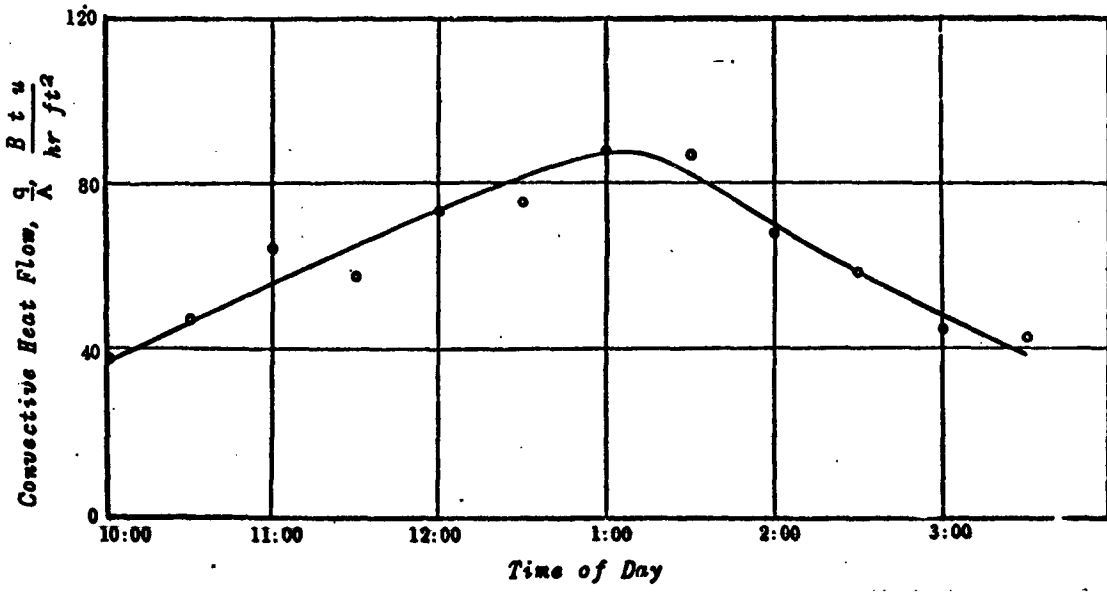


Figure 5. Vertical Convective Heat Transfer Versus Time .

also made under density flow conditions<sup>6</sup> between 6:44 A.M. and 6:54 A.M. Figure 6 shows a graph of shear stress as a function of wind velocity at the eighty inch level. The shear stress and velocity values were averaged over one to five minute time intervals. The afternoon shear stress data were noted to vary as the square of the velocity and were represented by equation (5); the drag coefficient was found to be 0.00137. This relation, which is noted as curve "A" in Figure 6, represents the data within an accuracy of  $\pm 30\%$ . Unfortunately the morning data consists of only two points. These points, however, are believed to be more accurate than some of the afternoon points because the stable air flow conditions at that time yielded very steady shear stress and wind velocity measurements. A square velocity relation faired through these two points and the origin is shown by curve "B" in Figure 6. It is intended that this curve suggest the effect of stability on the shear stress - wind velocity relation; many sets of data must be obtained before the stability effect can be thoroughly studied. The exponent on the common power wind velocity relation is about 0.16 for curve "A" and about 0.33 for curve "B". A calculation has revealed that if it were possible for completely laminar flow to exist under the existing velocity conditions, a shear-velocity curve falling far below curve "B" would result. If further research substantiates the above trend, it appears that for a given wind velocity, the atmospheric shear stress at the ground would increase with a decrease in the power law exponent (increased turbulence). This behavior would seem reasonable in the light of our present knowledge of fluid turbulence.

A comment on the height at which the wind velocity is to be measured and the accompanying implications seems to be in order. Consider the two velocity profiles shown in Figure 7; one profile is stable and one is unstable. Also consider that the stable profile is associated with a smaller shear stress than is the unstable profile.

---

<sup>6</sup>Nocturnal cooling of the earth's surface creates temperature inversions. An atmospheric system with such inversion conditions and sloping terrain then possesses a density potential which causes the cool air in the air layers contiguous to the ground to flow from higher to lower elevations.



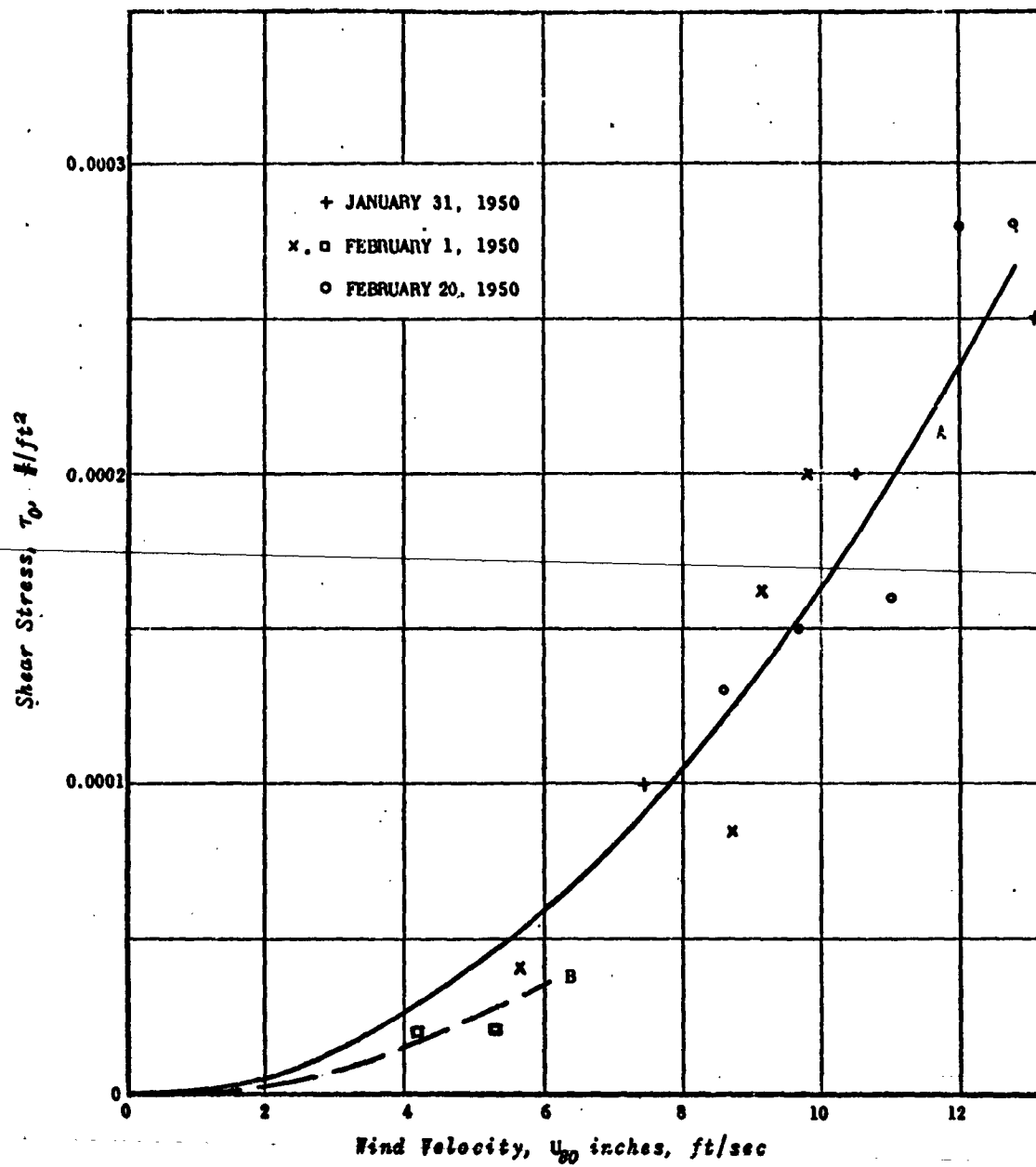


Figure 6. Shear Stress as a Function of Wind Velocity at 80 inches.

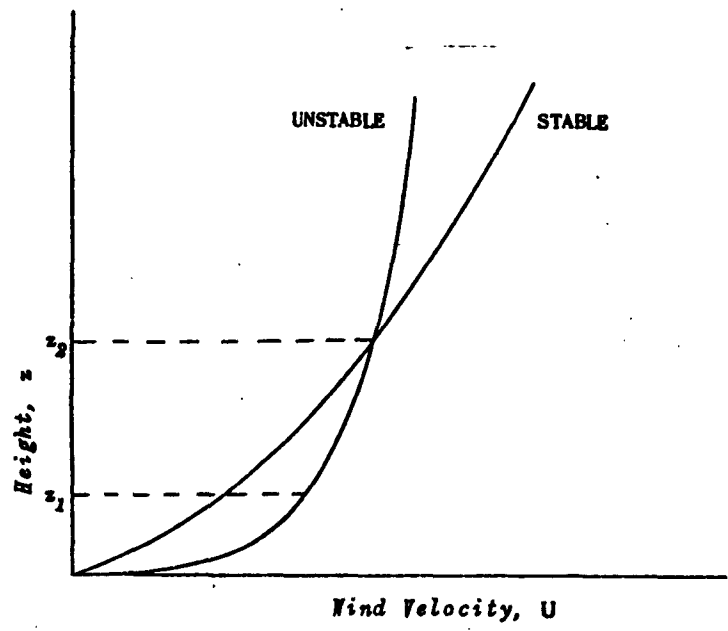


Figure 7. Stable and Unstable Wind Velocity Profiles

Consider the shear-velocity relations that result for each of the two proposed heights,  $z_1$  and  $z_2$  for the two velocity profiles shown. If  $z_2$  is chosen as the height at which the velocity is to be measured, it is seen that the stable shear stress is less than the unstable shear stress for the same wind velocity. However, if some lower reference height such as  $z_1$  is chosen, the stable velocity is so much less than the unstable one that the stable and unstable shear-velocity relations now may be much closer to each other than they were when the reference  $z_2$  was used. Further, if one chooses the reference height so that it lies within the laminar sub-layer, a single, linear shear-velocity curve would exist for stable, neutral, and unstable flow. That is, within the laminar sub-layer,

$$\tau_0 = \mu \frac{\delta U}{\delta z} = \mu \frac{U}{z} = \text{constant} \cdot U \quad (58)$$

A comparison of the Riverside shear data with some of the shear data reported in the literature is made in Figure 8. All velocities have been referred to a reference height of thirty feet. In some cases it was necessary to determine the velocity for the new reference height when complete velocity data were not reported; the seventh power velocity relation was utilized to make the determination.

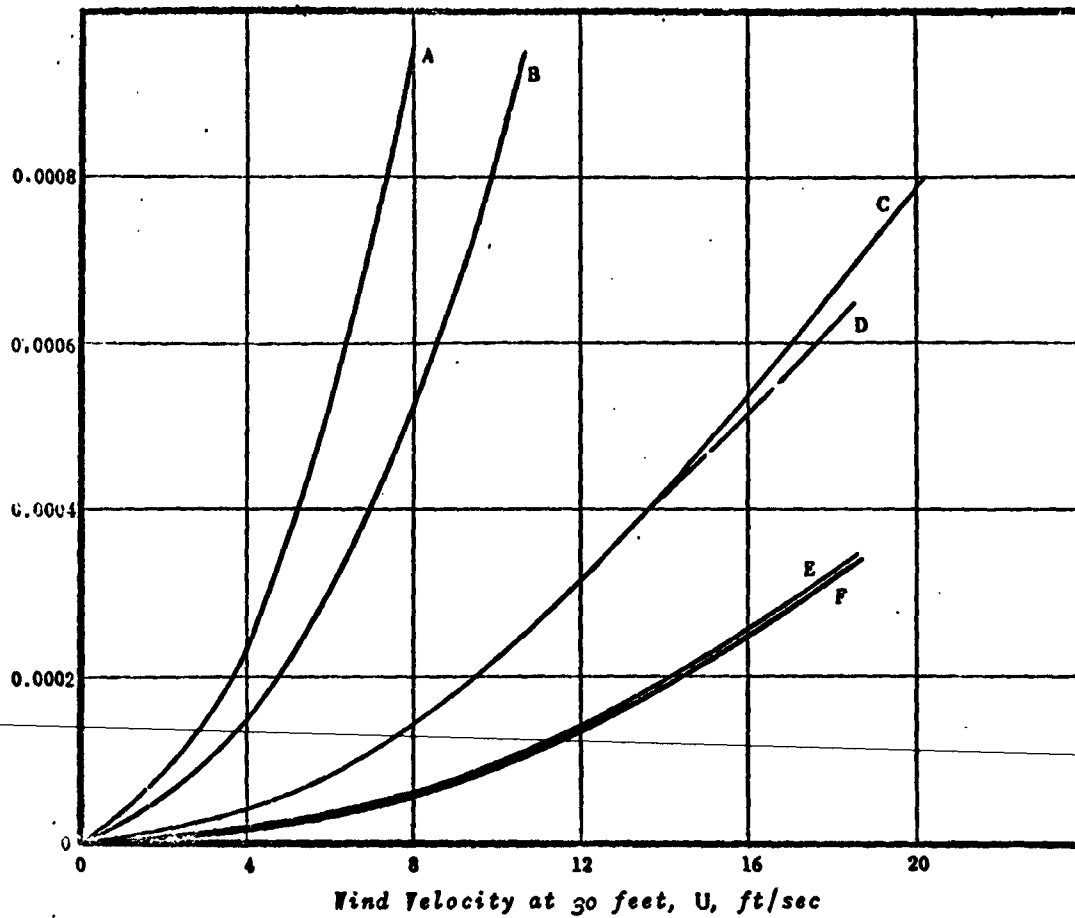
Sutcliffe and Taylor have utilized the technique of evaluating boundary shears from the hydrodynamic equations that describe the vertical wind spiral up to the gradient wind level; experimental vertical wind velocity measurements are necessary to make this determination. This method is predicated on the postulates that steady state flow conditions are established and that unidirectional flow exists at the earth's surface. Shear stresses calculated by this method represent mean values for the earth's surface and include the drag effects of such regions as bodies of water, plowed fields, brush land, orchards, and forests. Sutcliffe's data, curve "A", and Taylor's data, curve "B", which represent shear data over the Salisbury Plain, fall within forty percent of one another.

Sutcliffe also has obtained shear data over the South Atlantic with the aid of kites (see curve "E"); it seems reasonable that this curve should fall far below curves "A" and "B" because the ocean is a relatively smooth surface compared to land.

Curve "C" represents a shear-velocity relation which Rossby obtained by substituting experimental wind velocity data over the ocean into von Karman's generalized velocity distribution for flow in a smooth duct system.

The direct shear measurements of Sheppard with his shear meter are noted by Curve "D". These measurements were made over a smooth concrete surface.

It is of interest to compare Sheppard's results with those of the authors' as the flow systems were somewhat similar and because direct methods of measuring shear stress were used. It is suggested that Sheppard's data lie above the authors' data because of the difference in atmospheric stability in the two cases.



CURVE	INVESTIGATOR	SYSTEM	METHOD	EQUATION	REF.
A	Sutcliffe	Land Salisbury Plain	Pilot Balloon	$\tau_0 = 0.006 \rho U_{10}^2$	26
B	G. I. Taylor	Land Salisbury Plain	Pilot Balloon	$\tau_0 = 0.0025 \rho U_{30}^2$	27
C	Rossby	Sea Pacific	Empirical Duct Velocity Equations	$\tau_0 = 0.0008 \rho U_{16}^2$	28
D	Sheppard	Smooth Concrete Surface	Shear Meter	-	11
E	Sutcliffe	Average over No. So. Atlantic	Kites	$\tau_0 = 0.0004 U_{10}^2$	26
F	Authors	Flat, Disked Field	Shear Meter	$\tau_0 = 0.0004 U_{30}^2$	

Figure 6. A Comparison of Some of the Atmospheric Shear Stress Measurements Reported in the Literature

The velocity power law exponent for Sheppard's data was about 0.07 whereas the exponent for the author's data was about 0.16.

Momentum eddy diffusivities have been determined from the Riverside data with the aid of equation (2). The three typical profiles shown in Figure 9 indicate that the eddy diffusivity is approximately proportional to the wind velocity. Note that one can show from Prandtl's analytical, steady state, logarithmic, velocity solution that the eddy diffusivity is directly proportional to the velocity. Note also that these diffusivity profiles have configurations similar to those existing in the vicinity of the wall in duct flow systems; the diffusivity varies almost linearly with distance from a very small value (molecular viscosity) at the boundary.

#### B. Numerical Eddy Diffusion Analyses of Transient Air Temperature Data

Thermal eddy diffusivity profiles have been evaluated for two sets of transient air temperature measurements by means of numerical method No. 1 which has been described above. One set of data was obtained during a diffusion investigation in the desert at Datelan, Arizona, (Reference 29) and another set was obtained on gently rolling cotton land at Manor, Texas, (Reference 30).

Figure 10 shows some typical thermal eddy diffusivity profiles as a function of time for Datelan, Arizona. Calculations were not made for the late morning, noon, and early afternoon periods because atmospheric thermals existed at these times<sup>7</sup>. The diffusivity profiles in Figure 10 indicate the influence of the diurnal turbulence variation on convective heat transfer (high diffusivities during the day and low ones at night). The diffusivity profile at 0450 has been further sub-divided (note broken portion of curve) in order to show the influence of nocturnal stability on the diffusivity. The presence of this stable region was first suggested by the extreme temperature inversion conditions above the one hundred foot level. Note that all diffusivity profiles tend to pass through the origin. This characteristic appears to be an independent check on the diffusion analysis.

Comparisons of smoke diffusion in stable and unstable atmospheres at Datelan, Arizona, are made in Figure 11. Observe that the increased rate of vertical smoke

---

<sup>7</sup>A brief consideration of convective heat transfer in the presence of atmospheric thermals is given in the discussion section.

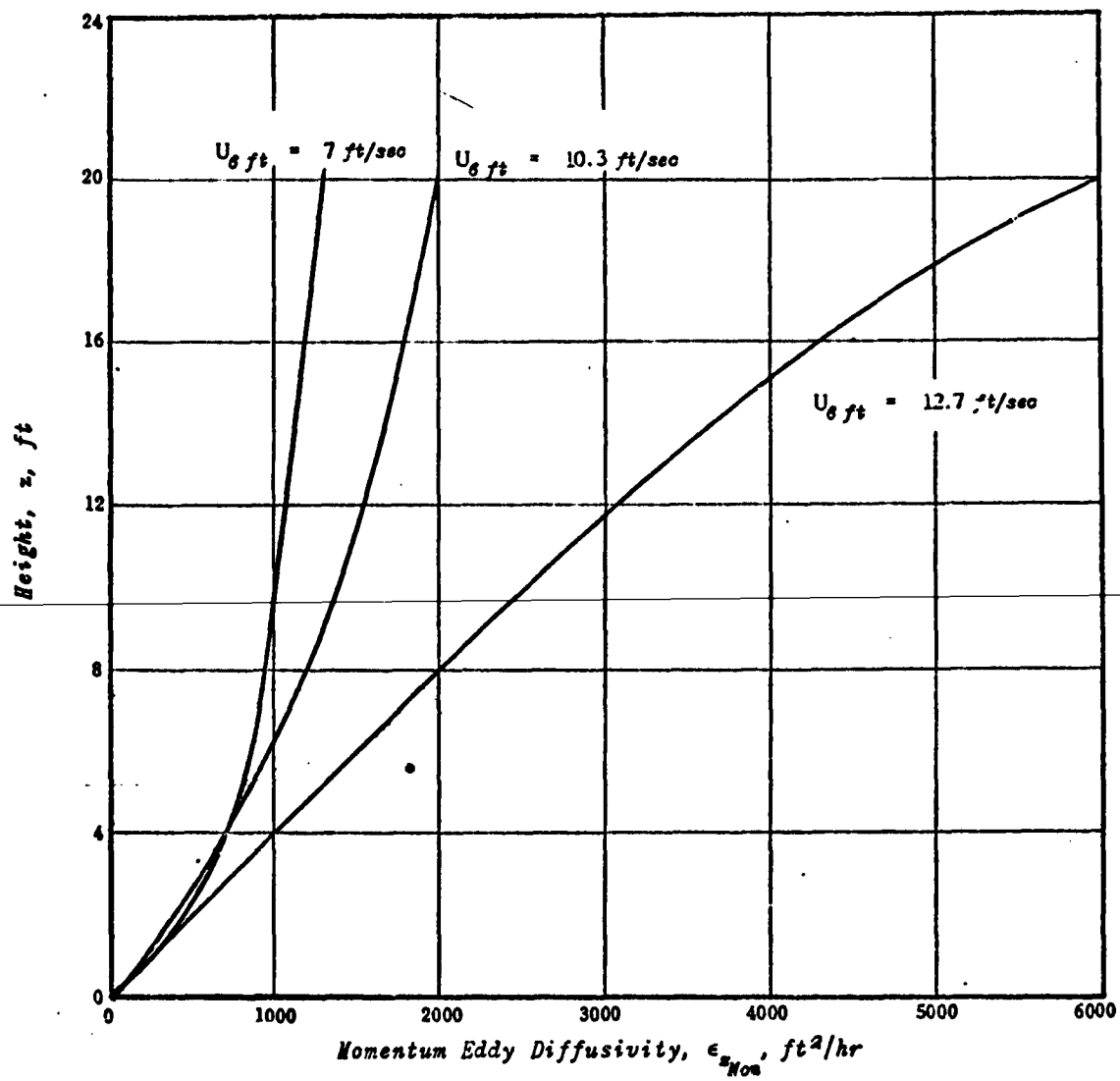


Figure 9. Momentum Eddy Diffusivity as a Function of Height,  
for Several Wind Velocities at Riverside  
(January, 1950)

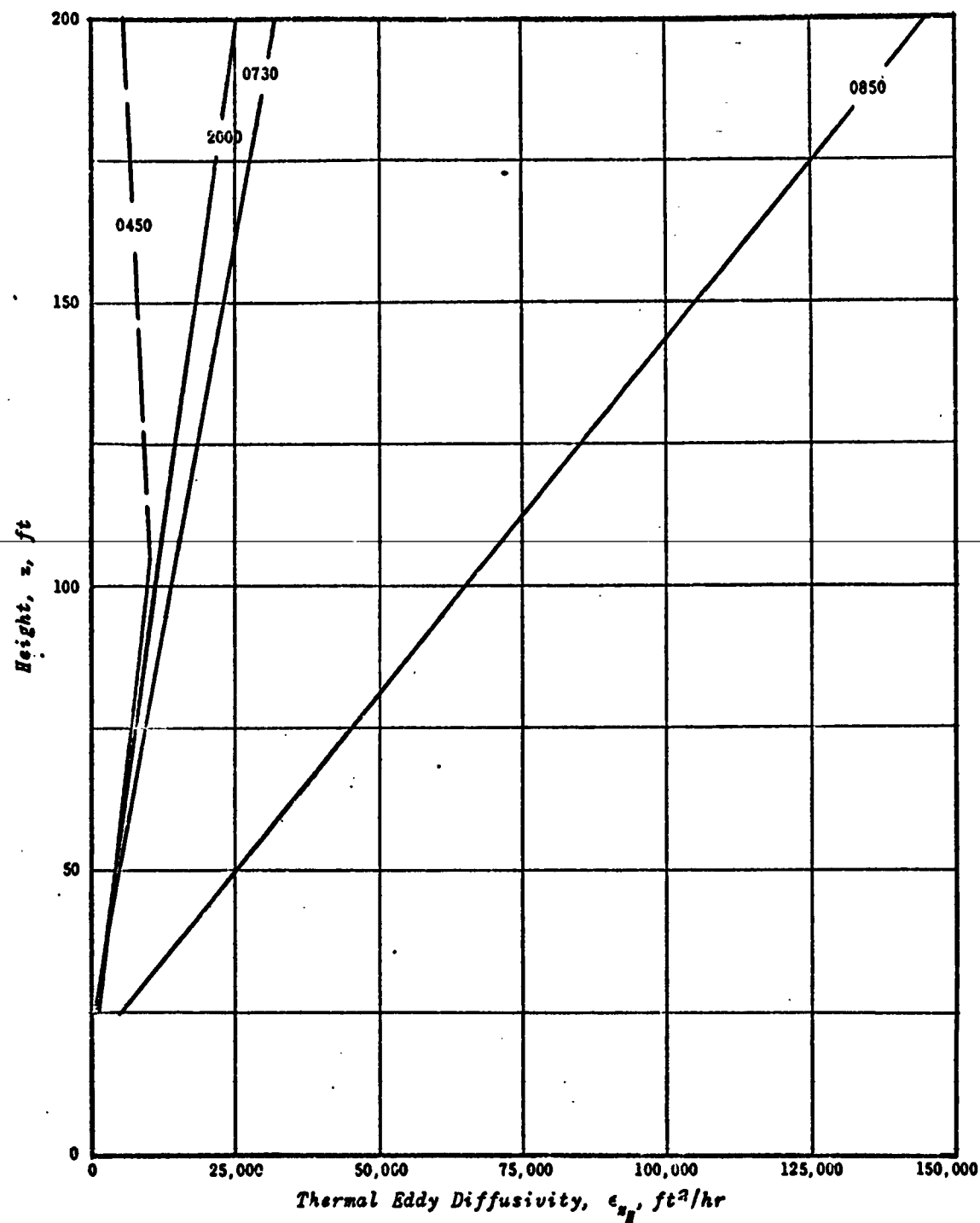


Figure 10. Vertical Thermal Eddy Diffusivity Profiles  
as a Function of Time at Datelan, Arizona  
(March, 1946)

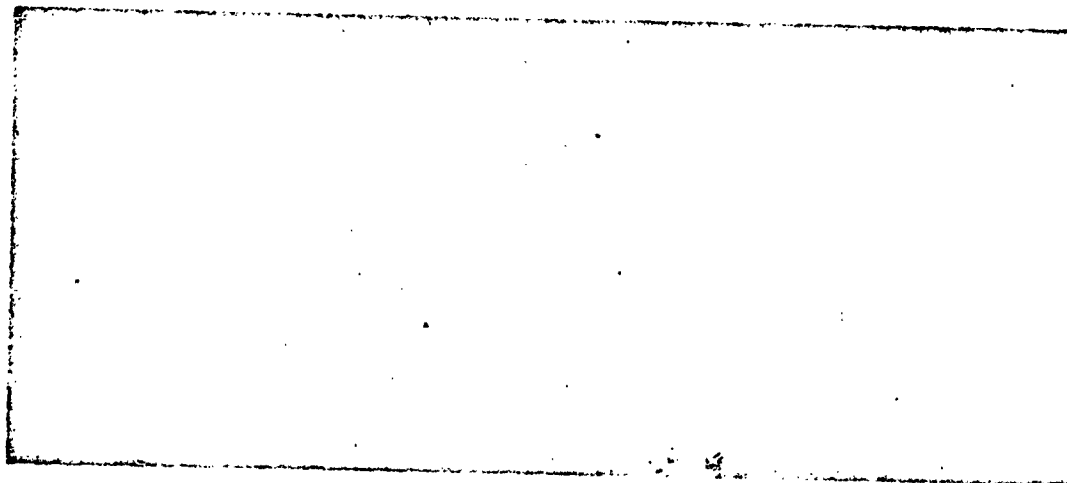


Stable Atmosphere

At  $z = 100'$ ,  $\epsilon_{zH} = 12,000 \text{ ft}^2/\text{hr}$

$U_{ave} = 4.5 \text{ mph}$

Time: 0730



Unstable Atmosphere

At  $z = 100'$ ,  $\epsilon_{zH} = 60,000 \text{ ft}^2/\text{hr}$

$U_{ave} = 4.0 \text{ mph}$

Time: 0850

Figure 11. Comparisons of Smoke Diffusion in a Stable and Unstable Atmosphere in Arizona



diffusion is in agreement with the increased eddy diffusivity at that time.

Figure 12 reveals day and night thermal eddy diffusivity profiles in the lower three hundred feet for Manor, Texas. The diurnal stability characteristics observed in the Arizona analysis are also noted in the Texas data.

#### C. Eddy Diffusion Analyses Found in the Literature

Some of the eddy diffusion analyses found in the literature are shown in Figures 13 and 14. Heat and momentum transfer diffusivity profiles in the lower twenty feet are presented in Figure 13. Curves B and C were deduced from Sheppard's shear stress and velocity data. Sheppard's diffusivity data are believed to fall above the Riverside data because of the more turbulent state of the atmosphere. Again note the important influence that wind velocity has on the magnitude of the eddy diffusivities.

A critical examination of the diffusion data given in Figures 13 and 14 has not been made because some of the pertinent parameters which are necessary to make such an examination were not reported in the literature. Also, some of the methods of analysis were not satisfactory.

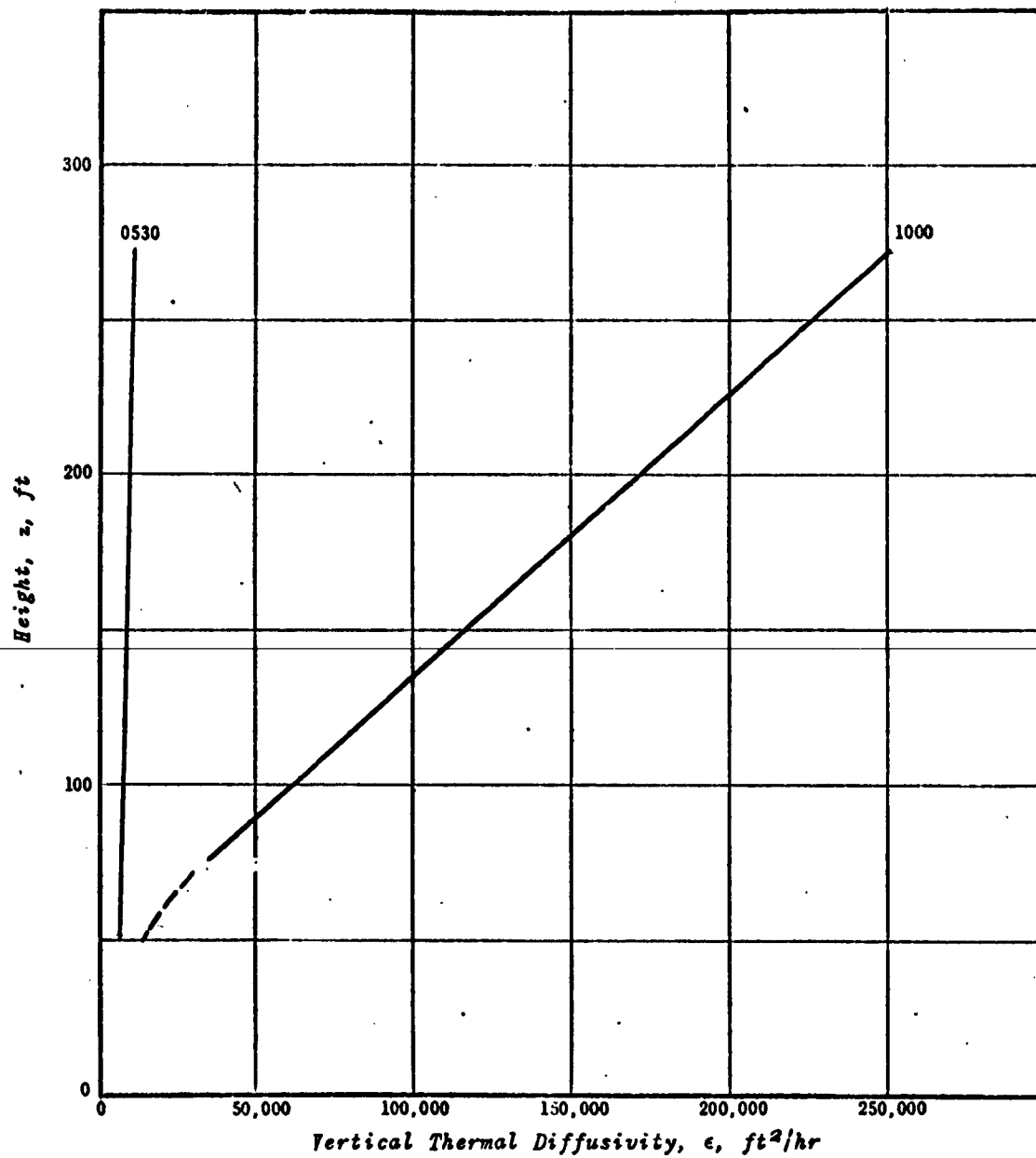
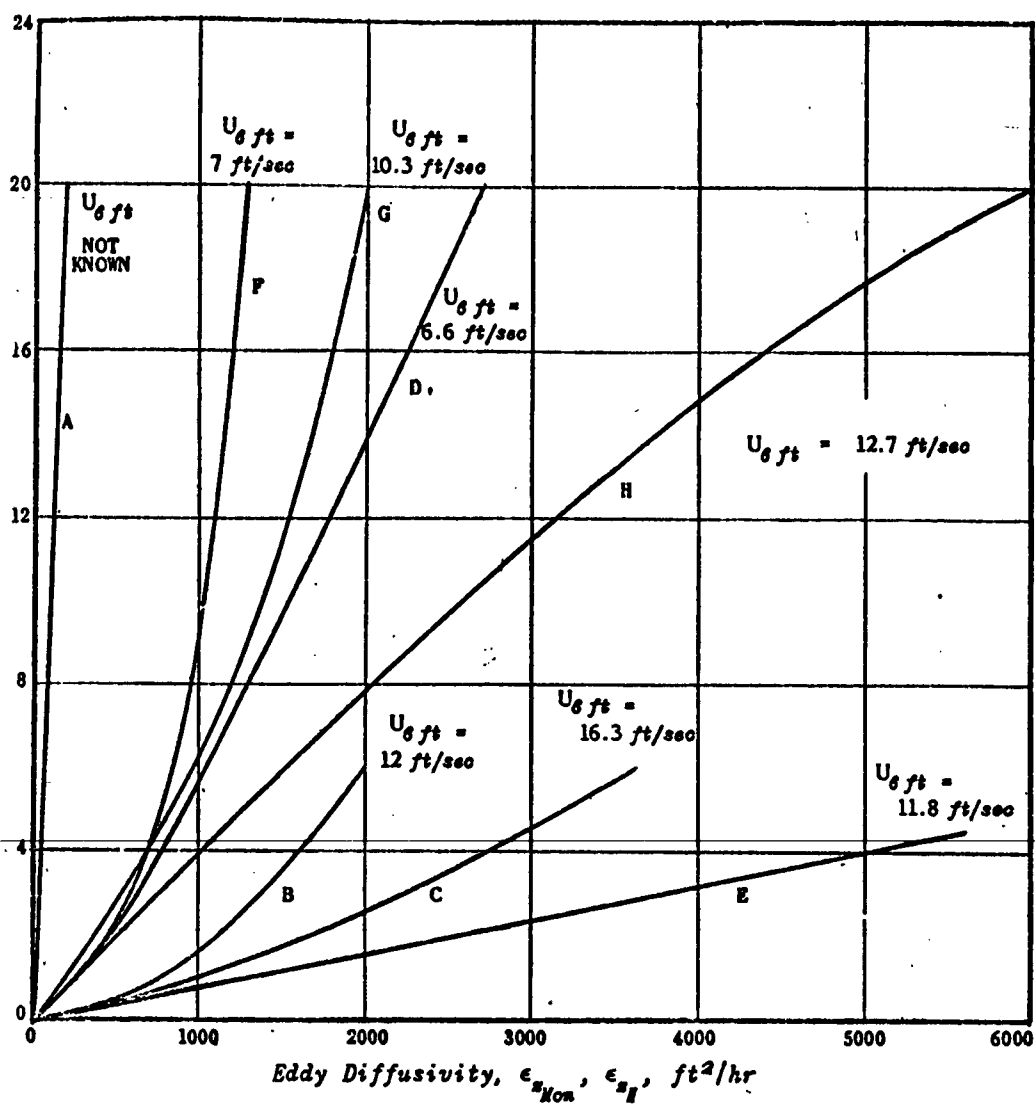


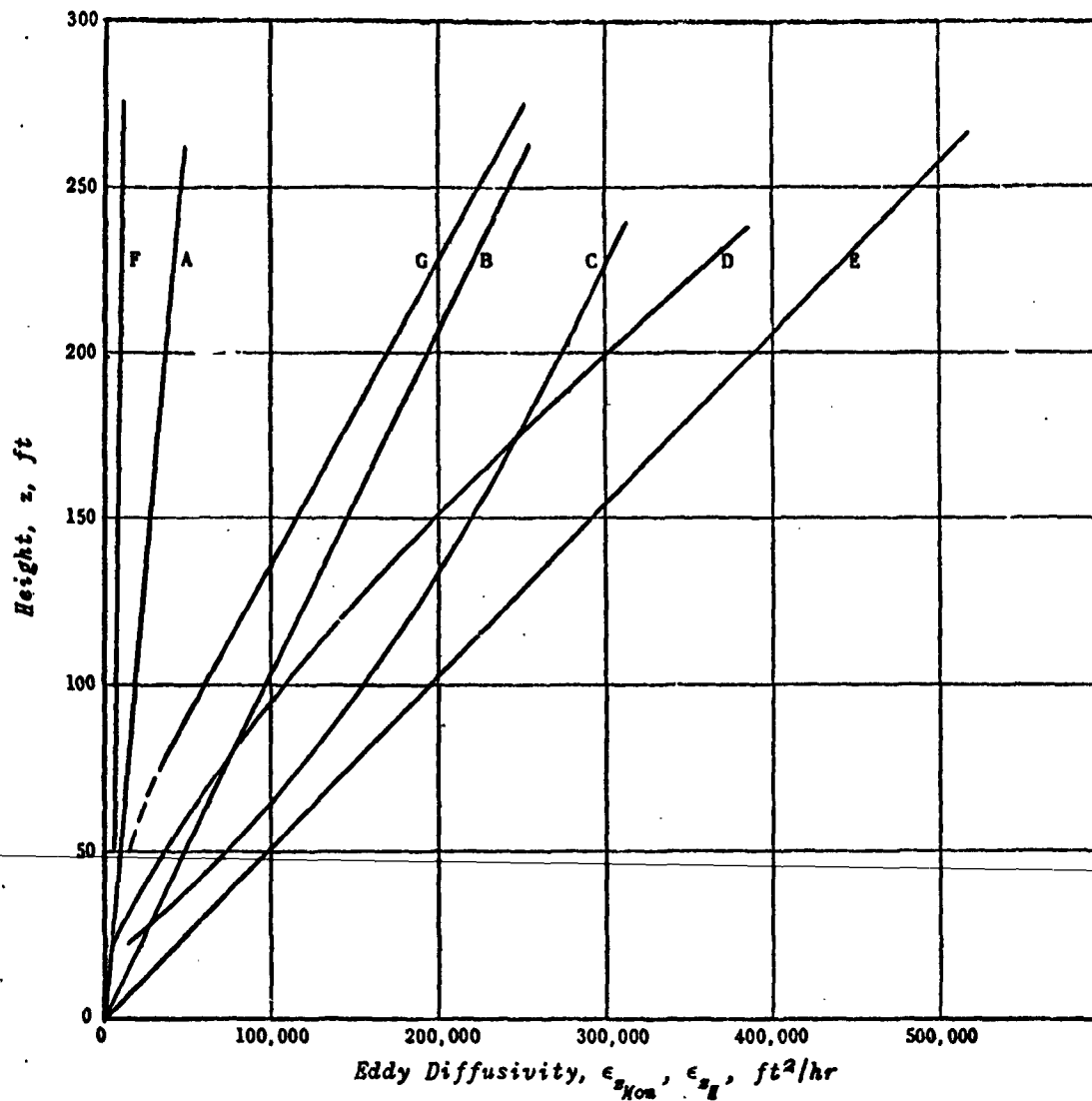
Figure 12. Vertical Thermal Eddy Diffusivity Profiles  
as a Function of Time at Manor, Texas  
(August, 1948)



CURVE	INVESTIGATOR	TRANSFER TYPE	LOCATION	REMARKS	METHOD	REF.
A	H. Berg	Heat	Moorland, Hannover	Day - Mean Values	Finite Difference Equation	21
B, C	Sheppard*	Momentum	Salisbury Plain	Day - Moderate Instability	$\epsilon = \frac{\tau_0}{\rho} \frac{1}{\delta U/z}$	11
D	Sverdrup	Heat	Icefield, Spitsbergen	Cold, Dry Weather	Heat Balance	14
E	Sverdrup	Heat	Icefield, Spitsbergen	Warm, Wet Weather	Heat Balance	
F, G, H	Authors	Momentum	Flat Field, Riverside	Day - Slight Instability	$\epsilon = \frac{\tau_0}{\rho} \frac{1}{\delta U/z}$	

\* Data analysed by authors

Figure 13. Some Eddy Diffusivity Profiles in the Lower 20 Feet of the Atmosphere Which Have Been Reported in the Literature



CURVE	INVESTIGATOR	TRANSFER TYPE	TIME	LOCATION	METHOD	REF.
A	Fritzsche, Stange	Heat	Night	Leipzig	Ertel's	31
B	Fritzsche, Stange	Heat	Day	Leipzig	Ertel's	
C	Johnson,	Heat	December	Lesfield, Oxon	Classical	32
D	Haywood	Heat	June	Lesfield, Oxon	Solutions	
E	Mildner	Momentum	Day	Leipzig	Solberg's	33
F	Authors	Heat	Night, 0530	Manor, Texas	Numerical	
G	Authors	Heat	Day, 1000	Manor, Texas	Method I	

Figure 14. Some Eddy Diffusivity Profiles in the Lower 300 Feet of the Atmosphere Which Have Been Reported in the Literature

## DISCUSSION

Investigators in the field of micrometeorology have questioned the use of the approximate eddy diffusion equations (which relate transfer rates to eddy diffusivities and potential gradients) under extremely unstable atmospheric conditions. Consider an unstable atmosphere in which large thermal convection patterns are in motion. It seems that vertical convective heat transfer should be expressed as the product of a vertical convective mass flow rate, a specific heat, and a difference in mean temperature of rising and falling air masses at a given elevation. Although some studies of convection patterns have been presented in the literature (Reference 34), attempts to solve the hydrodynamic and heat transfer equations simultaneously for the convection cell system should be made. However, if the vertical air velocities are not described by a regular convection pattern but consist of random fluctuations as in the case of stable, neutral, or slightly unstable flow, vertical heat, mass, and momentum transfer rates can be expressed by the eddy diffusion equations (1) and (2). These relations have satisfactorily been used in duct flow systems.

A simple heat-momentum transfer analogy<sup>8</sup> for the surface layer has been developed which relates some of the pertinent heat and momentum transfer variables that have been dealt with in this paper. The surface layer is postulated to consist of a laminar sublayer and a turbulent layer. The following table and figure give the heat and momentum transfer relations used in the derivation.

---

<sup>8</sup>This analogy, which is expressed in terms of dimensionless groups or moduli, is similar to the duct flow analogy developed by Boelter, Martinelli, and Jonassen (Reference 35).

TABLE I

Flow Region	Velocity Profile	Velocity Gradient	Shear Stress	Momentum Eddy Diffusivity	Thermal Eddy Diffusivity	Heat Flow
Laminar Sublayer: $0 < z < z_1$	$U = \frac{\tau_0}{\mu} z$	$\frac{\partial U}{\partial z} = \frac{\tau_0}{\mu}$	$\tau = \tau_0 = \mu \left( \frac{\partial U}{\partial z} \right)$	—	—	$\frac{q}{\lambda} = \left( \frac{q}{\lambda} \right)_0 = -k \left( \frac{\partial T}{\partial z} \right)$
Turbulent Layer $z > z_1$	$U = \sqrt{\frac{\tau_0}{\rho}} \frac{1}{K} \ln \frac{z + z_0}{z_0}$	$\frac{\partial U}{\partial z} = \frac{\tau_0}{\rho K} \frac{1}{(z + z_0)}$	$\tau = \tau_0 = \rho \epsilon_{MOM} \left( \frac{\partial U}{\partial z} \right)$	$\epsilon_{MOM} = \sqrt{\frac{\tau_0}{\rho}} K (z + z_0)$	$\epsilon_T = \alpha' \epsilon_{MOM}$	$\frac{q}{\lambda} = \left( \frac{q}{\lambda} \right)_0 = -\gamma c_p \epsilon_T \left( \frac{\partial T}{\partial z} \right)$

$z_1$  = laminar sublayer thickness

$z_0$  = reference height

$\mu$  = absolute air viscosity

$K$  = Karman constant, which in this case is a function of stability

$z_0$  = roughness boundary parameter, which is also a function of stability

$k$  = thermal conductivity of air

$$\alpha' = \frac{\epsilon_T}{\epsilon_{MOM}}$$

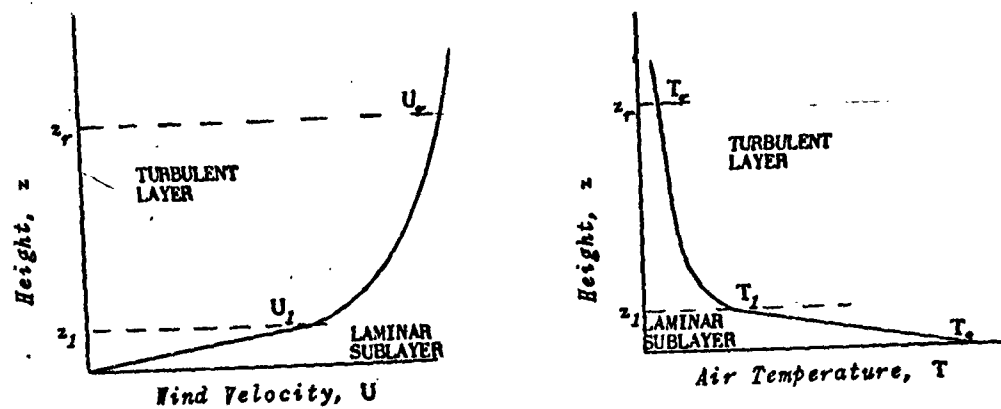


Figure 15. Velocity and Temperature Notations

It is possible to solve for the air temperature increments,  $(T_s - T_1)$  and  $(T_1 - T_r)$ , from the heat flow equations for the laminar and turbulent layers. These temperature increments can be substituted into the following defining equations for the unit thermal convective conductance (equation 4).

$$f_0 = \frac{\left(\frac{q}{A}\right)_0}{T_s - T_r} = \frac{\left(\frac{q}{A}\right)_0}{(T_s - T_1) + (T_1 - T_r)} \quad (4)$$

The following dimensionless moduli are defined

$$\left. \begin{aligned} Nu_r &= \frac{f_0 z_r}{k} \\ Re_r &= \frac{U_r z_r}{\nu} \\ z^+ &= \frac{z \sqrt{\rho_0}}{\nu} \\ Pr &= \frac{c_p \mu}{k} \end{aligned} \right\} \quad (59)$$

where,  $\nu'$  = kinematic viscosity  
 $g$  = acceleration of gravity

Upon the substitution of the temperature increments  $(T_s - T_1)$  and  $(T_1 - T_r)$  and the dimensionless moduli given by the equations (59) into equation (4), the following heat-momentum transfer analogy results:

$$Nu_r = \frac{\alpha' Re_r Pr \sqrt{g_0/\rho}}{U_r} \frac{1}{z_1' \left[ \alpha' Pr + \frac{1}{K z_1'} \ln \left( \frac{z_1' + z_0'}{z_1' + z_0'} \right) \right]} \quad (60)$$

It is sometimes desirable to express the shear stress in terms of the drag coefficient. Thus, equation (60) may be written as follows:

$$Nu_r = \frac{\alpha' Re_r Pr \sqrt{g_0/2}}{z_1' \left[ \alpha' Pr + \frac{1}{K z_1'} \ln \left( \frac{Re_r \sqrt{g_0/2} + z_0'}{z_1' + z_0'} \right) \right]} \quad (61)$$

Equation (60) or (61) relates the micrometeorological variables that describe the heat and momentum transfer processes within the surface layer. These variables are the 1) thermal conductance, 2) velocity at the reference height, 3) drag coefficient, 4) thickness of the laminar sublayer, 5) eddy diffusivity ratio,  $\alpha'$ , 6) fluid properties, and 7) the stability parameters  $K$  and  $z_0$ . The moduli  $Nu_r$ ,  $Re_r$  and the drag coefficient must all be expressed in terms of the same reference height,  $z_r$ , wherever it may be in the turbulent layer ( $z_r$  must be within the surface layer).

Experimental studies of all of the micrometeorological variables appearing in equation (61) are being conducted at the University of California. Some of these studies have been described in this paper; other studies involve the investigation of the following, under a range of stability conditions: 1) the laminar sublayer thickness for simple flow systems, 2) the parameter,  $\alpha'$ , from heat and momentum transfer measurements, and 3) the behavior of the stability and roughness parameters,  $K$  and  $z_0$ .



## ACKNOWLEDGEMENT

The authors wish to thank the following people  
who assisted in conducting the micrometeorological  
research described here:

F. A. Brooks

D. Rhoades

H. Schultz

R. Eldredge

R. Bromberg

## APPENDIX

Time	(q/A)solar $\frac{\text{Btu}}{\text{hr ft}^2}$	(q/A)cond. $\frac{\text{Btu}}{\text{hr ft}^2}$	(q/A)conv. $\frac{\text{Btu}}{\text{hr ft}^2}$	$\Delta t$ °F	$f_c$ $\frac{\text{Btu}}{\text{hr ft}^2 \text{ °F}}$	$U_5$ ft $\frac{\text{miles}}{\text{hr}}$
10:00	339	64	21	27	0.78	6.8
10:30	349	63	30	32	0.94	5.8
11:00	343	41	47	28	1.68	7.5
11:30	346	50	40	24.5	1.63	6.5
12:00	357	43	56	32	1.75	8.4
12:30	365	48	58	33.5	1.73	10.0
1:00	359	31	70	34	2.05	10.0
1:30	350	25	69	31	2.22	10.3
2:00	329	27	50	29	1.72	9.8
2:30	311	21	41	25	1.64	6.8
3:00	295	23	27	26	1.04	10.1
3:30	277	10	26	22	1.18	8.8

Table 2. Heat Flows, Temperature Differences, Wind Velocities, and Conductances for the Van Nuys Diffusion Study.

January 31, 1950		February 1, 1950		February 20, 1950	
$\tau_0$ lbs/ft <sup>2</sup>	U <sub>80 inches</sub> ft/sec	$\tau_0$ lbs/ft <sup>2</sup>	U <sub>80 inches</sub> ft/sec	$\tau_0$ lbs/ft <sup>2</sup>	U <sub>80 inches</sub> ft/sec
0.00025	12.9	0.0002	9.8	0.00028	12.7
0.0002	10.5	0.00016	9.1	0.00028	12.0
0.0001	7.4	0.000085	8.7	0.00016	11.0
		0.00004	5.7	0.00015	9.7
		0.000022	5.3	0.00013	8.6
		0.00002	4.2		

Table 3. Shear Stresses and Wind Velocities Obtained at Riverside

Z ft	U ft/sec	U ft/sec	U ft/sec	U ft/sec	U ft/sec	U ft/sec
0.167	4	6.25	1.4	1.6	4.5	4.1
0.75	5.65	9.4	2.4	2.9	---	---
1.62	6.3	---	---	---	---	---
3.25	6.7	11.65	3.7	4.6	8.7	7.9
6.67	7.1	12.9	4.1	5.3	9.1	8.7
13	8.6	13.9	5.0	5.4	9.5	9.2
20	9.3	14.4	5.3	5.7	9.9	9.6
Date	1/31/50	1/31/50	2/1/50	2/1/50	2/1/50	2/1/50
Time	2:30P	3:36P	6:54A	6:44A	2:43P	2:54P

Table 4. Some Wind Velocity Profiles for the Riverside

Diffusion Study

REFERENCES

1. Brunt, David,  
"Physical and Dynamical Meteorology," Cambridge University Press, London,  
1939, pg. 224.
2. Rouse, Hunter,  
"Fluid Mechanics for Hydraulic Engineers," McGraw-Hill Book Company, New York,  
1938, pgs. 169-188.
3. Goldstein, S.,  
"Modern Developments in Fluid Dynamics," Clarendon Press, Oxford, Vol. II,  
1938, pg. 647.
4. Rouse, Hunter,  
"Fluid Mechanics for Hydraulic Engineers," McGraw-Hill Book Company, New York,  
1938, pg. 179.
5. Martinelli, R. C., E. H. Morrin, and L. M. K. Boelter,  
NACA report: An Investigation of Aircraft Heaters "V - Theory and Use of Heat  
Meters For the Measurement of Rates of Heat Transfer Which Are Independent of  
Time," December, 1942.
6. Boelter, L. M. K., H. F. Poppendiek, and J. T. Gier,  
NACA report: An Investigation of Aircraft Heaters, "XIV - Experimental In-  
quiry into Steady State Unidirectional Heat Meter Corrections," ARR No. 4HO9,  
August, 1944.
7. Dunkle, R. V., T. T. Schimazaki, J. T. Gier, and L. Fossner,  
"Non-Selective Radiometers for Hemispherical Irradiation and Net Radiation  
Interchange Measurements," University of California, Department of Engineering,  
Berkeley, Contract No. N7-onr-295, Task 1, October, 1949.
8. Thornthwaite, C. W.,  
"Micrometeorology of the Surface Layer of the Atmosphere," Interim Reports  
No. 4 and 5 from The Johns Hopkins University, Laboratory of Climatology,  
October 1, 1948, December 1, 1949, March 31, 1949.
9. Martinelli, R. C.  
"Further Remarks on the Analogy Between Heat and Momentum Transfer," (a paper  
presented at The Sixth International Congress of Applied Mechanics, Paris,  
1946.
10. Sherwood, T. K., and B. B. Woerts,  
"The Role of Eddy Diffusion in Mass Transfer Between Phases," Transactions  
American Institute of Chemical Engineers, 35, 1939, pgs. 517-540.
11. Sheppard, P. A.,  
"The Aerodynamic Drag of the Earth's Surface and the Value of Von Karman's  
Constant in the Lower Atmosphere," Proceedings of the Royal Society of London,  
Vol. 188, Series A, 1946-47, pgs. 208-222.
12. Prandtl, L.,  
"Meteorologische Anwendung der Strömungslehre," Beiträge zur Physik der freien  
Atmosphäre, Bjerknes-Festschrift, Band 19, 1932, pgs. 188-202.

13. Rossby, C. G., and R. B. Montgomery,  
"The Layer of Frictional Influence in Wind and Ocean Currents," Papers in  
Physical Oceanography and Meteorology, Vol. III, No. 3, 1935.
14. Sverdrup, H. V.,  
"The Eddy Conductivity of the Air Over a Smooth Snow Field," Geofysiske  
Publikasjoner, Vol. XI, No. 7, 1936.
15. Lettau, H.,  
"Isotropic and Non-Isotropic Turbulence in the Atmospheric Surface Layer,"  
(a paper presented at a micrometeorological symposium at the University of  
California, Los Angeles, Feb. 7-8, 1949).
16. Sutton, O. G.  
"The Diffusive Properties of the Lower Atmosphere," Chemical Defense Experi-  
ment Station, Porton; M.R.P. No. 59, 1921-1942.
17. Brunt, David,  
"Physical and Dynamical Meteorology," Cambridge University Press, London,  
1939, pg. 229.
18. Haurwitz, B.,  
"The Daily Temperature Period for a Linear Variation of the Austausch  
Coefficient," Transactions of the Royal Society of Canada, Vol. XXX,  
Series 3, 1936, pgs. 1-12.
19. McLachlan, N. W.  
"Bessel Functions For Engineers," Oxford University Press, London, 1946,  
pg. 170.
20. Longley, R. W.,  
"The Evaluation of the Coefficient of Eddy Diffusivity," Quarterly Journal  
of the Royal Meteorological Society, Vol. 70, No. 306, 1944, pgs. 286-291.
21. Berg, H.,  
"Messungen der Austauschgrößen der bodennahen Luftschichten," Beiträge zur  
Physik der freien Atmosphäre, Band 23, Heft 1-4, 1936, pgs. 143-164.
22. Vehrencamp, J. E.  
A research report for the Department of Engineering, University of California,  
Los Angeles, September, 1949.
23. Boelter, L. M. K., and J. T. Gier,  
"The Silver-Constantan Plated Thermopile," Temperature - Its Measurement  
Control in Science and Industry, Reinhold Co., 1941, pgs. 1284-1292.
24. Boelter, L. M. K., H. F. Poppendiek, G. Young, and J. R. Andersen,  
NACA report: "An Investigation of Aircraft Heaters," XXX - Nocturnal  
Irradiation as a Function of Altitude and Its Use in Determination of Heat  
Requirements of Aircraft," TN 1454, January, 1949.
25. Brooks, F. A., and C. F. Kelly,  
"Instrumentation for Recording Microclimatological Factors," (a paper pre-  
sented at the American Geophysical Union, Section of Meteorology, Meeting at  
Davis, California, Feb. 1950.)
26. Sutcliffe, R. C.,  
"Surface Resistance in Atmospheric Flow," Quarterly Journal of the Royal  
Meteorological Society, Vol. 62, 1936, pgs. 3-14.

27. Taylor, G. I.,  
"Skin Friction of the Wind on the Earth's Surface," Proceedings of the Royal Society of London, A92, 1915-16, pgs. 196-199.
28. Rossby, C. G.,  
"On the Momentum Transfer at the Sea Surface," Papers in Physical Oceanography and Meteorology, Vol. IV, No. 3, 1936.
29. Boelter, L. M. K., H. F. Poppendiek, G. Young, D. C. Nelson, and H. A. Johnson,  
Smoke Studies Report for the Bureau of Ships, Contract NObs 2490, July 1, 1946.
30. Gerhardt, J. R., K. H. Jehn, W. R. Guild, and R. C. Staley, "Micrometeorological Research Data," Electrical Engineering Research Laboratory, University of Texas, Contract No. N6onr-266, Task II, Volume 1, November 1948.
31. Fritzsche, G., and R. Stange,  
"Vertikalen Temperaturverlauf über einer Großstadt," Beiträge zur Physik der freien Atmosphäre, Band 23, Heft 1-4, 1936, pgs. 95-110.
32. Johnson, N. K., and G. S. P. Heywood,  
"An Investigation of the Lapse Rate of Temperature in the Lowest Hundred Meters of the Atmosphere," Meteorological Office Geophysical Memoirs, Vol. IX, No. 77, 1938.
33. Mildner, P.,  
~~Über die Reibung in einer speziellen Luftmasse in den untersten Schichten der Atmosphäre,~~ Beiträge zur Physik zur freien Atmosphäre, Band 19, 1932, pgs. 151-158.
34. Brunt, David,  
"Physical and Dynamical Meteorology," Cambridge University Press, London, 1939, pg. 220.
35. Boelter, L. M. K., R. C. Martinelli, and Finn Jonassen,  
"Remarks on the Analogy Between Heat Transfer and Momentum Transfer," American Society of Mechanical Engineers, Transactions, July 1941, pgs. 447-455.